

Dear Editor,

On behalf of my co-authors, we thank you very much for your kind work and anonymous reviewers' constructive comments on our manuscript entitled "Characterization of atmospheric trace gases and particle matters in Hangzhou, China" (acp-2017-777) published in ACPD as scientific article. These comments are all valuable and helpful for revising and improving our paper, as well as the important guiding significance to our researches. We have studied the comments carefully and made corresponding corrections in the revised manuscript. We hope that this revision could meet the requirement of ACP.

Here we have to clarify two significant corrections in the revised manuscript.

1) The first is that we have to change the corresponding author's address from the initial version of zhangg@camsma.cn to the new one of zhanggen@cma.gov.cn because the original email address is about to expire due to the new regulation of our institute.

2) The second is that we changed the initial manuscript name as the new version of "Characterization of atmospheric trace gases and **particulate** matters in Hangzhou, China" in the revised manuscript, according to the comment recommended by anonymous referee.

The referees' comments and our response point by point are listed below.

Thank you for your time in advance.

Sincerely,

Dr. Gen Zhang (E-mail: zhanggen@cma.gov.cn)

Zhongguancun South Str. 46, Haidian District,

Chinese Academy of Meteorological Sciences (CAMS),

Beijing 100081, China

Response to Anonymous Referee #1

This manuscript reports one-year continuous measurements of trace gases and particulate matters at a National Reference Climatological Station in Hangzhou, southern Yangtze River Delta region. The data were analyzed in terms of seasonal variations, interspecies correlations, and potential contributions from local emissions and regional transport. The measurement data of the present study are much valuable, and the analysis and interpretation of the data are fairly well. Thus, it is recommended that this manuscript can be considered for publication after the following comments being addressed.

Response: Thanks for your recognition and positive comments on our manuscript. According to your suggestions, we made the corresponding corrections in the revised manuscript. We expect this version would meet the requirement for publication in ACP.

Specific Comments:

1. Overall, the interpretation and analyses of the measurement results are fairly well, but there is lack of comparison with the other studies and importance or implications of the present study. To date there have been many measurement studies in the YRD region, such as at Lin'an, Shanghai and Nanjing. The authors should point to the new findings or difference between this new piece of work and the previous studies.

Response: Thank you very much for the suggestions about making comparison with the other studies. As depicted in the revised manuscript, we have elaborated more examples about the knowledge gap between this work and the previous studies and further pointed out our new finding.

2. The first paragraph of the Introduction section contains a lot of very basic information on the individual trace gases. I presume that the readership of the Journal should be expertise of this field, and suggest the authors to remove (or shorten) such general description and just focus on the key knowledge gaps and motivation of the study in the Introduction part.

Response: Yes, you are right. According to your comments, we removed some basic introduction related to the well-known trace gases including NO_x, CO, and SO₂ in the first paragraph in the revised manuscript.

3. Page 2, Line 52: intermediates/products

Response: As you suggested, we made corrections as “intermediates/products” in the revised manuscript.

4. Page 2, Line 55: and/or

Response: As you suggested, we replaced it with “and/or” in the revised manuscript.

5. Page 3, Lines 80-81: it is not clear what the “large knowledge gap and discrepancy” means. Please

elaborate more about the knowledge gap.

Response: Thanks for your valuable comments about “large knowledge gap and discrepancy”. As mentioned in Response 2 above, we elaborated more examples about the knowledge gap in the revised manuscript.

6. Line 3, Line 89: Experiment and meteorological conditions

Response: Thanks for your valuable comments about “large knowledge gap and discrepancy”. As mentioned in Response 2 above, we elaborated more examples about the knowledge gap in the revised manuscript.

6. Line 3, Line 89: Experiment and meteorological conditions

Response: In the revised manuscript, we changed it with “Experiment and meteorological conditions” as you suggested.

7. Line 3, Line 93: please provide the standard deviations for the average temperature, RH and rainfall.

Response: Thanks for your mention on this expression to improve our manuscript. As you suggested, we added the standard deviations for the average air temperature and RH. However, as shown in Table 1, we used the accumulated monthly value for rainfall (not the average) and thus it has no standard deviations.

8. Section 2.1: the authors need clearly state the type (e.g., urban, suburban or rural) of the study site.

What are the major emission sources surrounding the site?

Response: We have stated the type of our study site (urban site) in the revised manuscript. With respect to the major emission sources surrounding this site, we have made the specific introduction as below in the revised manuscript.

“As a typical urban site, NRCS station is situated in the commercial and residential areas in the southern Hangzhou and thus it’s characterized as a polluted receptor site as it receives local urban plumes and regional air masses from the YRD region when northwesterly wind prevails. In addition, as the right top map shown in Fig. 1, the site is adjacent to Prince Bay Park (area, 0.8 km²) and situated in the northeastern part of West Lake famous scenic spot (area, 49 km²). Therefore it can also capture the signature of vegetation emission in urban Hangzhou under southwesterly winds. Moreover, there are no local industrial pollution sources around the site. In brief, this site can be representative of urban Hangzhou.”

9. Section 2.2, on the measurements of NO₂ and CO: what kind of converter was used for the conversion from NO₂ to NO? Is there auto-zero or auto-reference function for the CO analyzer, and what is the time frequency for the auto-zeroing during the campaign?

Response: Your suggestions are very important and valuable. In our study, we used internal and external MoO converter for the conversion from NO₂ and NO_z to NO, respectively. For CO analyzer,

there was auto-zero function and its time frequency was every 6 h during the campaign. The corresponding corrections were made in the revised manuscript, as shown below.

“NO and NO_x were detected by a chemiluminescence analyzer coupled with an internal MoO catalytic converter (TEI, 42i). Note that the differentiated value of NO₂ from NO_x and NO represents the upper limit concentration of atmospheric NO₂ due to the interference of other nitrogen-containing components (e.g., PAN, HNO₃, and HONO) in the conversion. Similar with NO_x, NO_y was also detected by a chemiluminescence analyzer (TEI 42i-Y) but equipped with an external MoO catalytic converter. CO was monitored with a gas filter correlation, infrared absorption analyser (TEI, 48i), with automatic zeroing every 6 hours.”

14. Page 7, Lines 188-191: some studies have also investigated the seasonal variations of O₃ in Hong Kong and North China, and the authors should acknowledge these earlier studies.

Response: As you suggested, we have added the two earlier studies in the revised manuscript.

15. Page 7, Line 192: Xianlin?

Response: Yes, you are right. We are sorry for this mistake. This site is “Xianlin”

16. Page 8, Lines 227-228: revise this sentence

Response: According to your comment, we have changed this sentence with “In summer (Fig. 2f), an abnormally high level of O_x was found in winter with low O₃.” in the revised manuscript.

17. Page 9, Line 257: color-coded

Response: According to your comment, we have replaced “coded” with “color-coded” in the revised manuscript.

18. Page 9, Line 258: led to

Response: According to your comment, we have replaced it with “led to” in the revised manuscript.

19. Page 9, Line 275: change “in addition to” to “in view of”

Response: According to your comment, we have changed “in addition to” with “in view of” in the revised manuscript.

20. Page 10, Line 297: pay attention to

Response: According to your comment, we have replaced it with “pay attention to” in the revised manuscript.

21. Page 11, Lines 329-330: why the air masses coming from open seas contained higher concentrations of NO_x and O₃? The authors need elaborate more about the reason for this interesting result.

Response: At first, we are so sorry for the incorrectly expression “long transports from Yellow Sea, East Sea, and South Sea were also important potential sources for NO_x and O₃” in the initial manuscript. After careful examination, we found that air masses with the seemed high WPSCF values for NO_x were not originating far from these open seas. They were just the broadening “tails” of high values contained in the areas with intensive anthropogenic NO_x emissions from inland well-industrialized cities. This phenomenon was also found in other studies by using trajectory statistical method (Riuttanen et al., 2013).

Similar with NO_x, air masses containing the high WPSCF values of O₃ also didn't come from the open seas. Indeed, as depicted in the manuscript, such air masses were mostly from the offshore area of East China Sea, Yellow China Sea, or South China, respectively on southeastern Zhejiang, Jiangsu, and Fujian Province. We speculated the recirculation of pollutants by sea- and land-breeze circulations around the cities along the YRD and Hangzhou Bay which has been confirmed by Li et al. (2015, 2016b), was largely responsible for the increased concentration of O₃ at NRCS site.

Also, such an increase in O₃ concentrations in urbanized coastal areas have been observed and modeled in a number of studies (Oh et al., 2006; Levy et al., 2008; Martins et al., 2012). Moreover, to further judge whether air masses came from open seas contained higher concentrations of NO_x and O₃, we used the results of MOZART-4/GEOS-5 simulation to draw the distribution maps of NO_x and O₃ concentrations within the identical domain (15-55 °N and 105-135 °E) with WPSCF analysis. As clearly seen from the Figure 1 below, high NO_x mainly distributed in terrestrial regions, especially in industrialized cities, but very low NO_x were found in open seas. In comparison, significantly high O₃ were elucidated covering the offshore regions of either East China Sea, Yellow China Sea, or South China Sea (Fig. 2). Then, along with the seasonal cluster analysis of back trajectories from NRCS site in Hangzhou, it's well confirmed that our speculation about the contribution of the recirculation of pollutants by sea- and land-breeze circulations in the offshore area to the observed O₃ at NRCS site.

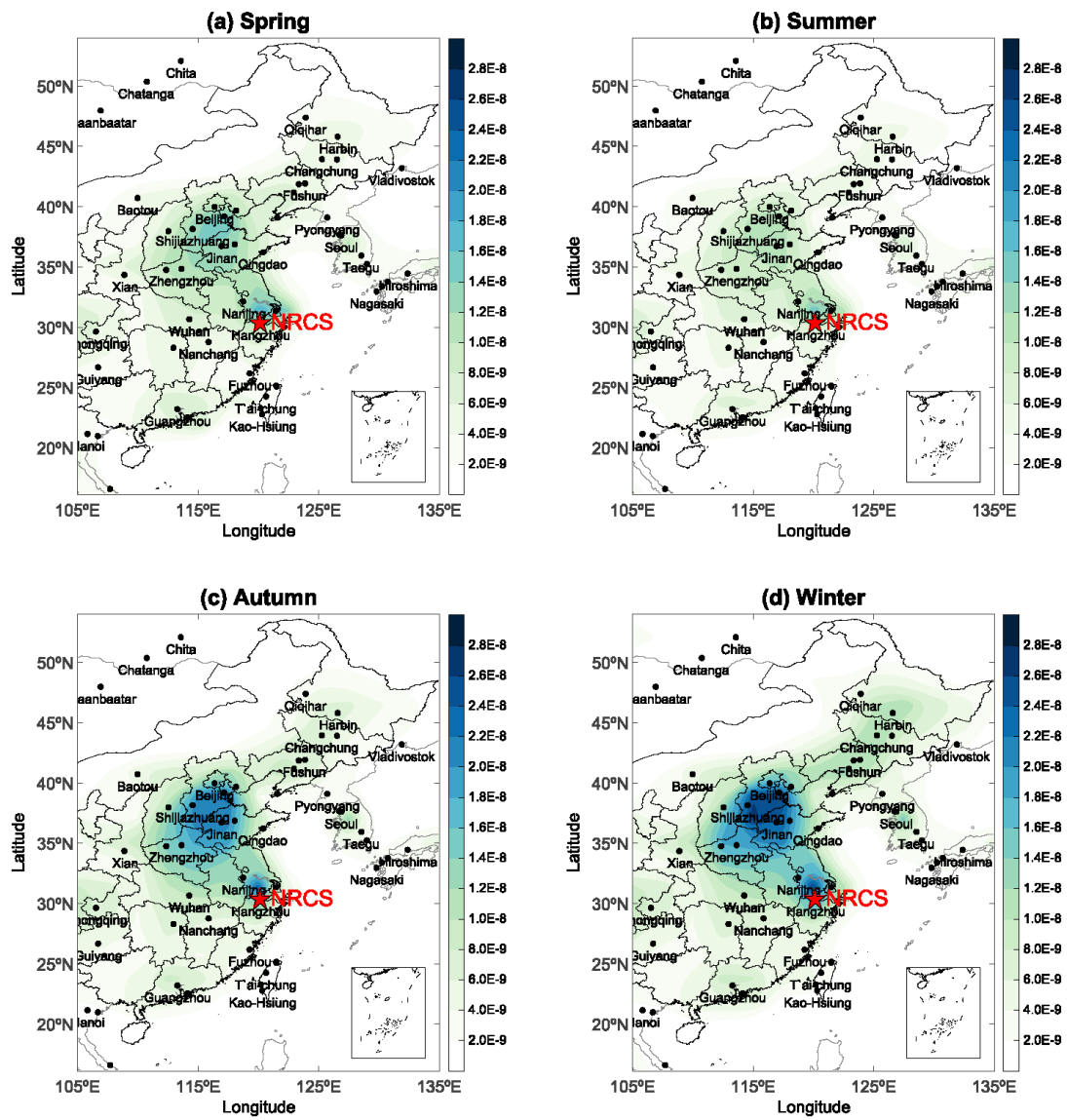


Figure 1 Seasonal and spatial distributions of NO_x volume mixing ratio (VMR) simulated by MOZART-4/GEOS-5. The sample site is marked in pentacle.

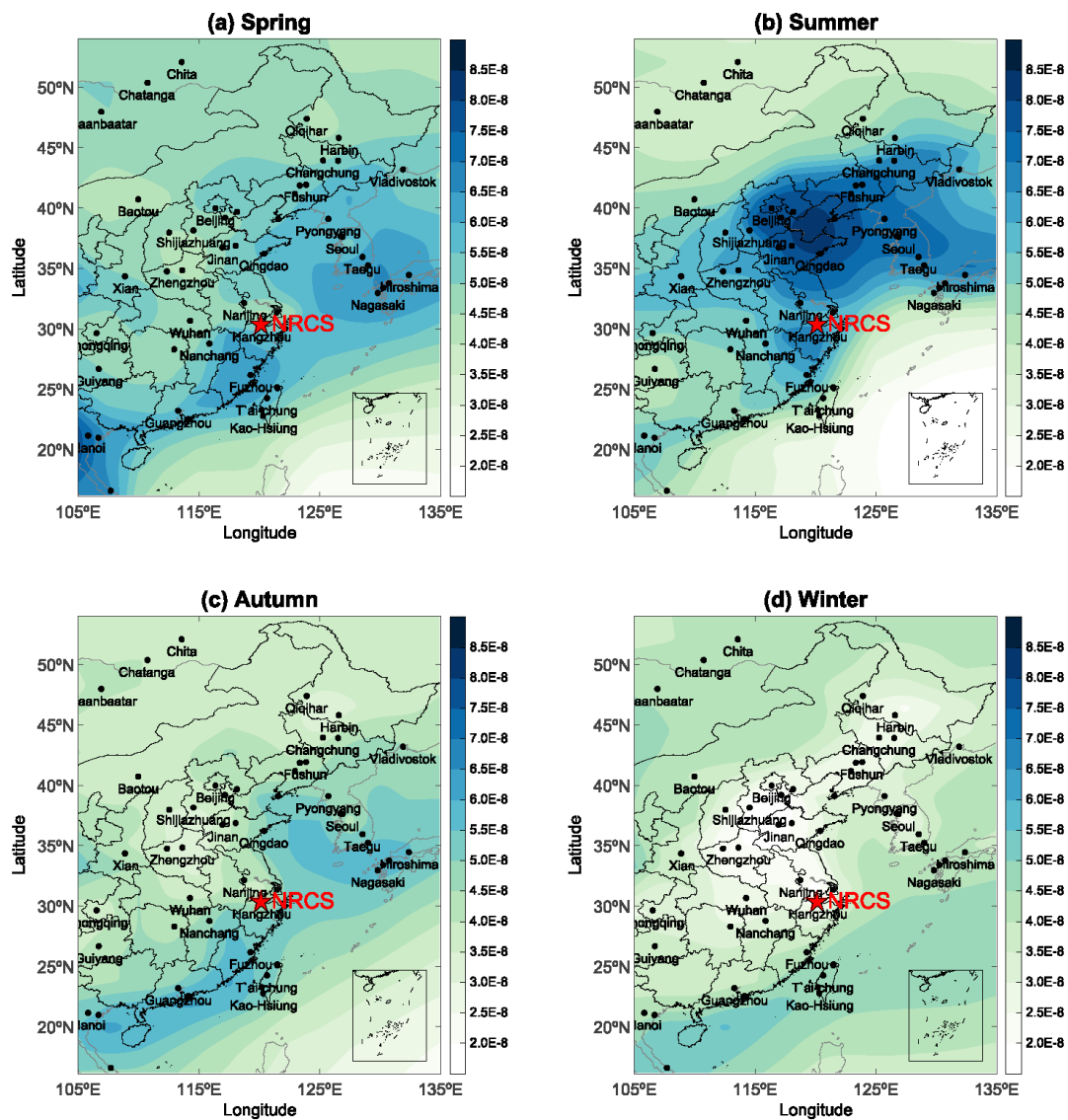


Figure 2 Seasonal and spatial distributions of O₃ volume mixing ratio (VMR) simulated by MOZART-4/GEOS-5. The sample site is marked in pentacle.

Reference

- Levy, I., Dayan, U., and Mahrer, Y.: A five-year study of coastal recirculation and its effect on air pollutants over the east Mediterranean region, *J. Geophys. Res.*, 113, D16121, 2008.
- Li, M. M., Mao, Z. C., Song, Y., Liu, M. X., and Huang, X.: Impact of the decadal urbanization on thermally induced circulations in eastern China, *J. Appl. Meteorol. Clim.*, 54, 259-282, 2015.
- Li, M. M., Song, Y., Mao, Z. C., Liu, M. X., and Huang, X.: Impact of thermal circulations induced by urbanization on ozone formation in the Pearl River Delta, China, *Atmos. Environ.*, 127, 382-392, 2016b.
- Martins, D. K., Stauffer, R. M., Thompson, A. M., Knepp, T. N., and Pippin, M.: Surface ozone at a coastal suburban site in 2009 and 2010: relationships to chemical and meteorological processes, *J. Geophys. Res.*, 117, D5, 5306, 2012.
- Oh, I. B., Kim, Y. K., Lee, H. W., and Kim, C. H.: An observational and numerical study of the effects

of the late sea breeze on ozone distributions in the Busan metropolitan area, Korea, *Atmos. Environ.*, 40, 1284-1298, 2006.

Riuttanen, L., Hulkkonen, M., Dal Maso, M., Junninen, H., and Kulmala, M.: Trajectory analysis of atmospheric transport of fine particles, SO₂, NO_x and O₃ to the SMEAR II station in Finland in 1996-2008, *Atmos. Chem. Phys.*, 13, 2153-2164, 2013.

22. Page 12, Line 359: long distance transport

Response: According to your comment, we have replaced it with “long distance transport” in the revised manuscript.

23. Figures 3-7: it would be better to combine these figures into one figure.

Response: According to your comment, we have combined the four figures, the scatter plots of NO_y-O₃ coded with air temperature (a), NO_y-PM_{2.5} coded with relative humidity (b), NO_y-SO₂ coded with relative humidity (c), and O₃-PM_{2.5} coded with air temperature (d), into one figure as Fig. 3 shown in the revised manuscript. In order to facilitate the clear view of the subpicture showing the scatter with O₃ mixing ratios above 80 ppbv, we keep the scatter plots of NO_y with CO in a single figure as Fig. 4 shown in the revised manuscript.

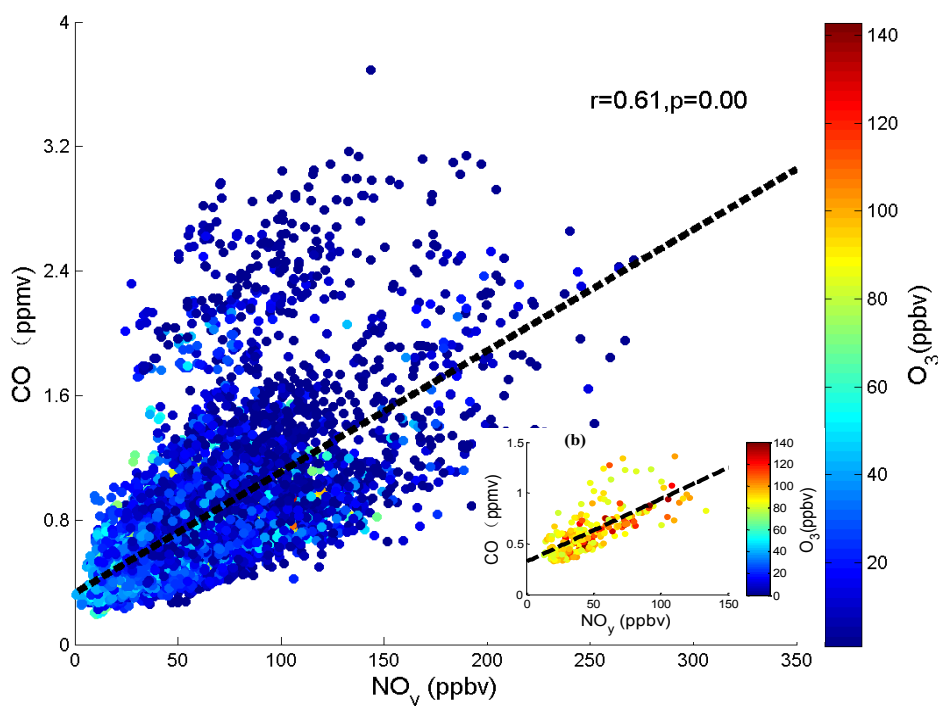


Fig. 4. Scatter plots of NO_y with CO coded with O₃ mixing ratios, along the subpicture (b) showing the scatter with O₃ mixing ratios above 80 ppbv.

Response to Anonymous Referee #2

The manuscript ‘Characterization of atmospheric trace gases and particle matters in Hangzhou, China’ by G. Zhang et al. reports the observational results from one-year monitoring of several trace gases and particulate matter at an urban site in the YRD region. The characteristics of these trace gases and particulate matter are discussed in association with meteorological conditions. Process analysis is also performed for case studies under photochemical pollution and haze condition. The measurement data are valuable, but the manuscript needs to be more concise and more logically structured. Further proofreading is also needed to correct grammar mistakes and inappropriate description.

Response: Thanks for your approval and presenting the valuable comments on our manuscript. According to your suggestions, we restructured our manuscript logically, shortened some redundant description and corrected grammar mistakes in the revised version. We expect this version would meet the requirement for publication in ACP.

Specific comments:

1. ‘Particle matter’ is used almost through the entire manuscript, it should be particulate matter.

Response: According to your suggestion, we replaced “particle matter” with “particulate matter” in the revised manuscript.

2. Was the air sample dried when measuring PM_{2.5}? How about the drying system?

Response: As described in the manuscript, ambient PM_{2.5} samples were collected using co-located Thermo Scientific (formerly R&P) Model 1405D samplers. This sampler has no dried unit in our study.

3. What is the temporal resolution of the meteorological data in the HYSPLIT model? Will the temporal resolution and also the spatial resolution as $0.5^{\circ} \times 0.5^{\circ}$ influence your conclusions?

Response: As described in Section 2.4.1 in the manuscript, the six hourly final archive data with $1^{\circ} \times 1^{\circ}$ spatial resolution were obtained from the National Center for Environmental Prediction’s Global Data Assimilation System (GDAS) wind field reanalysis. Such designated data have been widely used in numerous previous studies (Li et al., 2015; Yu et al., 2014; Zhang et al., 2013). As you know, the numbers of back trajectories starting from a selected site during the appointed period are probably dependent of temporal and spatial resolution of the meteorological data. Nevertheless, the trajectory cluster analysis is based on the statistical results of air masses back trajectories, and it should don’t change a lot. Thus they don’t lead to a significant effect on the conclusion.

References:

Li, P. F., Yan, R. C., Yu, S. C., Wang, S., Liu, W. P., and Bao, H. M.: Reinstatement regional transport of PM_{2.5} as a major cause of severe haze in Beijing, Proc. Natl. Acad. Sci., 112(21), 2739-2740, 2015.

Yu, S. C., Zhang, Q. Y., Yan, R. C., Wang, S., Li, P. F., Chen, B. X., Liu, W. P., and Zhang, X. Y.: Origin of air pollution during a weekly heavy haze episode in Hangzhou, China, *Environ. Chem. Lett.*, 12, 543-550, 2014.

Zhang, R., Jing, J., Tao, J., Hsu, S. C., Wang, G., Cao, J., Lee, C. S. L., Zhu, L., Chen, Z., Zhao, Y., and Shen, Z.: Chemical characterization and source apportionment of PM_{2.5} in Beijing: seasonal perspective, *Atmos. Chem. Phys.*, 13, 7053-7074, 2013.

4. P9 L246-249, the author suggested comparable photochemical levels in different regions only based on measurements of NO₂ and O₃, I am afraid it is insufficient to draw this conclusion.

Response: After careful examination throughout the manuscript, we didn't find these sentences in this version of the manuscript. These sentences were possibly included in the previous version and have been removed in this version.

5. The discussion on NO_x or VOCs limitation of ozone photochemical production is based on measured CO. The author stated that VOCs and CO share common origins and play similar roles in ozone production in this region. Is there any data or previous study in this region to support this assumption?

Response: For VOCs and CO in the typical urban regions, their common origin and similar behavior in ozone production have been explicitly elucidated (Atkinson, 2000) and widely validated in the previous studies (Baker et al., 2008; Schneidemesser et al., 2010; Ding et al., 2013). Moreover, based on the data of VOCs and CO obtained at Lin'an site, a regional station located in the east Zhejiang Province (50 km away from Hangzhou) in eastern China, Guo et al. (2004) found the common sources of VOCs and CO were vehicle emissions and biofuel burning, biomass burning and industrial emissions. In addition, we Therefore, we added the previous publications behind this sentence to support our assumption in the revised manuscript.

References:

Atkinson, R.: Atmospheric chemistry of VOCs and NO_x, *Atmos. Environ.*, 34, 2063–2101, 2000.

Baker, A. K., Beyersdorf, A. J., Doezema, L. A., Katzenstein, A. K., Meinardi, S., Simpson, I. J., Blake, D. R., and Rowland, F. S.: Measurements of nonmethane hydrocarbons in 28 United States cities, *Atmos. Environ.*, 42, 170-182, 2008.

Ding, A. J., Fu, C. B., Yang, X. Q., Sun, J. N., Zheng, L. F., Xie, Y. N., Herrmann, E., Nie, W., Petäjä, T., Kerminen, V. M., and Kulmala, M.: Ozone and fine particulate in the western Yangtze River Delta: an overview of 1 yr data at the SORPES station, *Atmos. Chem. Phys.*, 13, 5813-5830, 2013.

Guo, H., Wang, T., Simpson, I. J., Blake, D. R., Yu, X. M., Kwok, Y. H., and Li, Y. S.: Source contributions to ambient VOCs and CO at a rural site in eastern China, 38(27), 4551-4560, 2004.

6. The correlations of O₃ and PM_{2.5} in warm and cold seasons were analyzed. The author attributed the positive correlation in warm seasons to secondary aerosol formation under high O₃ levels and negative

correlation in cold seasons to NO titration effect. However, the ambient level of either O₃ or PM_{2.5} is a result of emission, sinks, physical processes and complicated chemical reactions. The explanation has no solid foundation and also needs other supporting data.

Response: Your suggestions are really valuable. Unfortunately, in this study we didn't conduct the chemical elements, ion, and OC/EC analysis of particulate matters and thus no available data could directly support this assumption. However, we find another reliable evidence based on the available data of the observed PM_{2.5} and gaseous pollutants in our measurement to support our conclusion. To judge whether the secondary aerosol formed during the warm seasons and was further related with high O₃ concentrations, we chose two typical O₃ exceedances (OE) cases under air temperature on 10 and 12 July (OE1: 95 ppbv for average O₃ and 35.9 °C for average T) and 10-11 August (OE2: 92.7 ppbv for average O₃ and 38.7 °C for average T), respectively, together comparison with their nearby non-O₃ exceedances periods (NOE) from 7-8 July (NOE1) and 13-14 August (NOE2). Note that these data were both selected as the time period of 9:00-17:00 BLT, to reflect the photochemistry as possible. As can be seen from Table 1 below, the average PM_{2.5} concentrations in OE1 and OE2 were both higher (ca. 2-4 folder) than those in NOE1 and NOE2, respectively. It suggested a significant formation of PM_{2.5} in the OE event. Furthermore, to further distinguish the primary and secondary contribution to PM_{2.5}, we compared the ratio of the averaged PM_{2.5} concentrations in OE to that in NOE events ($PM_{2.5(OE)}/PM_{2.5(NOE)}$) with the ratios for other gaseous pollutants. If the ratio of $PM_{2.5(OE)}/PM_{2.5(NOE)}$ was comparable with that for other primary pollutants, it probably indicated that a significant contribution of primary particulate matter to the observed PM_{2.5} in OE event. As clearly shown in Table 1, the ratios of $PM_{2.5(OE1)}/PM_{2.5(NOE1)}$ and $PM_{2.5(OE2)}/PM_{2.5(NOE2)}$ were 2.08 and 4.12, respectively, both higher than those for the other primary gaseous pollutants during these two episodes (1.20-1.61 and 1.62-2.58), indicating a significant contribution of secondary particulate matter to the observed PM_{2.5} in warm seasons.

Table 1 Average concentrations of PM_{2.5} and gaseous pollutants and their average ratios in the O₃ exceedances period on 10 and 12 July (OE1) and 10-11 August (OE2), and the nearby non-O₃ exceedances period from 7-8 July (NOE1) and 13-14 August (NOE2), respectively.

Species	Same time period (9:00-17:00 BLT)					
	OE1*	NOE1*	OE1/NOE1	OE2*	NOE2*	OE2/NOE2
PM _{2.5}	50.65	24.36	2.08	41.96	10.17	4.12
O ₃	95.43	53.23	1.79	92.69	42.71	2.17
SO ₂	12.73	7.89	1.61	5.18	2.01	2.58
CO	0.46	0.38	1.20	0.48	0.30	1.62
NO _y	35.72	23.95	1.49	29.30	16.22	1.81

* $\mu\text{g}/\text{m}^3$ unit for PM_{2.5}, ppmv unit for CO, and ppbv unit for the other gases, respectively

In addition, we find other simultaneous/previous observations implemented in urban Hangzhou to support our supposition. Sun et al. (2013) conducted an intensive field campaign in Hangzhou during

Sep. 2010-July 2011 and found that molar ratios of sulfate to total sulfur and nitrate to total oxidized nitrogen frequency exceeded 10%, suggesting significant effects of photochemical reactions on PM_{2.5} pollution in the urban Hangzhou. Thus, secondary particulate formation may be related to high conversion rate of SO₂ and NO_x to sulfate and nitrate under a high concentration of oxidants (Khoder, 2002; Sun et al., 2013). Note that it's necessary to implement more detailed investigations related with chemical elements, ion, and OC/EC analysis of particulate matters.

In the revised manuscript, we made corresponding corrections as mentioned above.

References:

Khoder, M. I.: Atmospheric conversion of sulfur dioxide to particulate sulfate and nitrogen dioxide to particulate nitrate and gaseous nitric acid in an urban area, *Chemosphere*, 49, 675-684, 2002.

Sun, G. J., Yao, L., Jiao, L., Shi, Y., Zhang, Q. Y., Tao, M. N., Shan, G. R., and He, Y.: Characterizing PM_{2.5} pollution of a subtropical metropolitan area in China, *Atmos. Climate Sci.*, 3, 100-110, 2013.

7. The backward trajectory and PSCF analysis is not suitable for short-lived species such as O₃ and is especially not suitable in urban area with high local emission. So it's strange that those clean mountain area in south of Hangzhou could have more contributions? As well as that air masses coming from open seas contained higher concentrations of NO_x and O₃?

Response: We thank the referee for his/her valuable comments. We divide this comment into four questions in details:

1) The backward trajectory and PSCF analysis is not suitable for short-lived species such as O₃

At first, we have to clarify that this WPSCF analysis has its limitation. In principle, it's just a statistical method correlating air masses origin with the pollutants concentrations measured in a selected site. We agree with referee that the PSCF analysis used for so-called short-lived species such as O₃ might add uncertainty to our results, but it will not lead to the wrong results. The method is based on the theory that those map grid cells that get much "probability" of high concentration will have an increased importance in the source area maps. A significant area will get more "probability" when a trajectory passes it again but from a slightly different direction when the length of air masses trajectory was longer than life time of the pollutant. Areas behind the source areas will have smeared concentration probability and will be mixed also with clean trajectories that have gone around the source area, thus it might arise broadening "tails" behind the significant source area with high concentration. Similar phenomenon was also found in other studies by using trajectory statistical method (Riuttanen et al., 2013).

However, this method also has significant advantage. It is a useful, widely-used, and simple way to see

where the higher concentrations (relative to a set value) come from, and thus it could represent the potential/relative source contribution fields. As mentioned in the Response 3 above, this method has been employed to elucidate the potential source contributions of particulate matters. In addition, apart from the application in investigating the potential source contributions of the trace gases such as SO₂, CO, and NO_x (Kaiser et al., 2007; Riuttanen et al., 2013; Yu et al., 2014), it has been increasingly applied to identify the origin of O₃ pollution (Stohl and Kromp-Kolb, 1994; Dickerson et al., 1995; Poirot and Wishinski, 1998; Kaiser et al., 2007; Riuttanen et al., 2013; Vellingiri et al., 2016; Sharma et al., 2017), and even extended to a more complicatedly secondary pollutant of atmospheric peroxyacetyl nitrate (PAN) (Siroris and Bottenheim, 1995). As you know, O₃ has variable precursors and complex sink mechanisms. In fact so complex that a statistical method such as PSCF has been proven to perform better compared to deterministic trajectory based method (Schlink et al., 2003). Therefore, this method has been validated to be suitable not only for particulate matters but also for trace gases such as O₃, SO₂, CO, and NO_x.

2) The backward trajectory and PSCF analysis is especially not suitable in urban area with high local emission.

With respect to the applicability of this method in urban area, we have to clarify again that it just provides a general indication of the potential source probability areas **in statistical sense** and thus it's free of turbulence, dry and wet deposition, and chemical reactions (Kaiser et al., 2007). The back trajectory and PSCF method have been widely used in the analysis of atmospheric NO₂ and O₃ in urban Hangzhou (Wu et al., 2016) and the other typical urban sites in Toronto and Montreal in eastern Canada (Johnson et al., 2007), Naples in southern Italy (Riccio et al., 2007), Korea (Vellingiri et al., 2016), and New Delhi (Sharma et al., 2017). Even, this method could be used to assess the effects of transboundary ozone pollution between Ontario, Canada and New York (Brankov et al., 2003). For NRCS site, a typical urban site located in Hangzhou, it is an ideal receptor to capture the mixed signature of local emission and regional transport, with the short and long cluster-mean trajectories, respectively.

3) So it's strange that those clean mountain area in south of Hangzhou could have more contributions?

To answer the question about high contribution from the south of Hangzhou, we first view the terrain and geographical distribution in Zhejiang Province. For Zhejiang Province, its terrain inclines from southwest to northeast, and geographically many cities (i.e., Shaoxing, Jinhua, Lishui, and Quzhou city) located in the south of Hangzhou. High O₃ is expected to be produced in these urban regions and carried to the NRCS site by the dominant southwesterly wind. Thus these areas could act as potential source regions. In addition, we think that biogenic VOCs (BVOCs) emitted from the mountain area in the south of Hangzhou might play a certain role in the formation of local O₃ during the whole year except

winter. This supposition was well evidenced by seasonal and spatial distributions of O₃ volume mixing ratio (VMR) simulated by MOZART-4/GEOS-5 (See the Figure 1 below). Clearly shown in this figure, high concentrations of O₃ distributed in the south of Hangzhou including the mountain area during the whole year except winter.

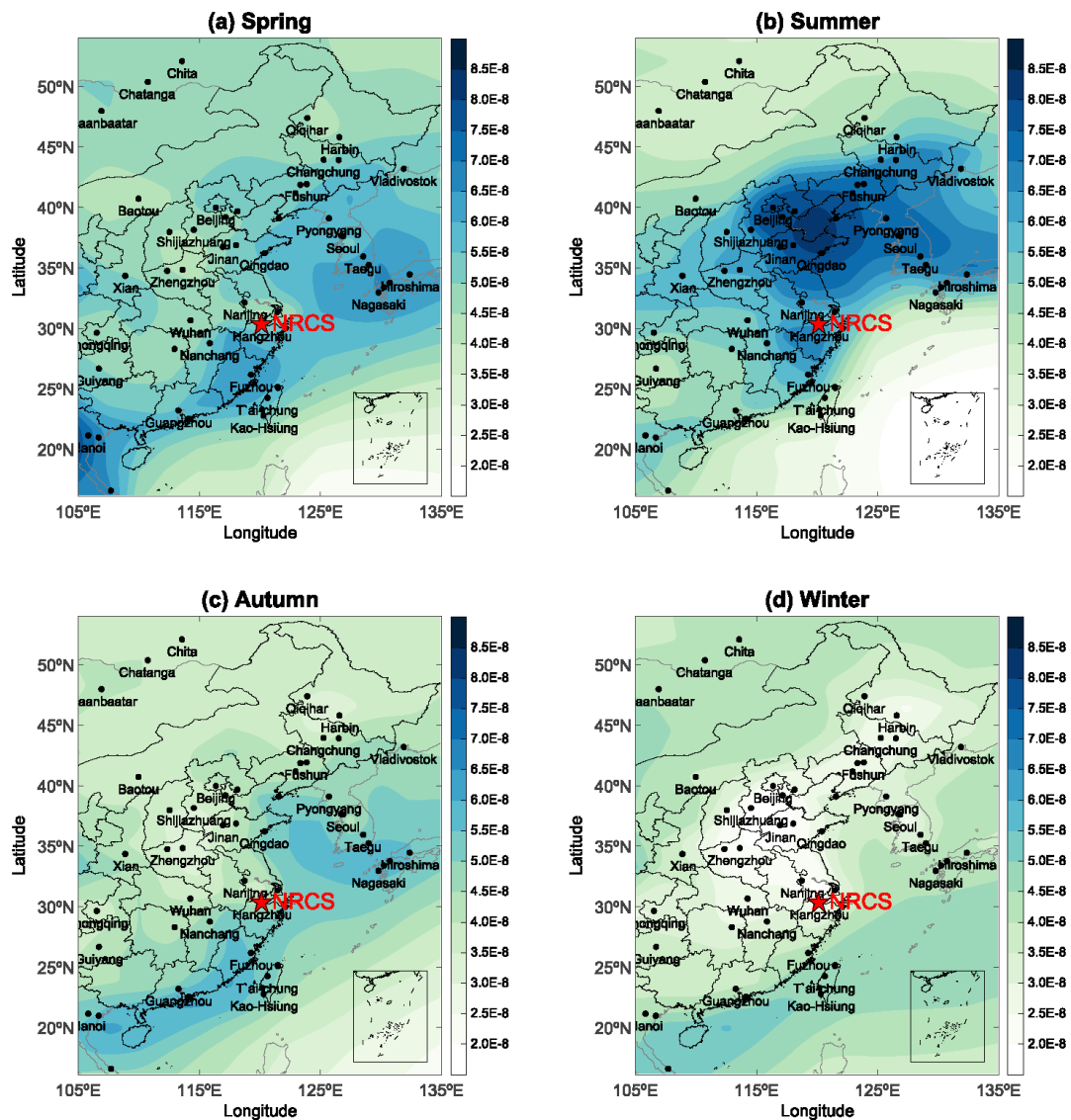


Figure 1 Seasonal and spatial distributions of O₃ volume mixing ratio (VMR) simulated by MOZART-4/GEOS-5. The sample site is marked in pentacle.

4) As well as that air masses coming from open seas contained higher concentrations of NO_x and O₃?

As responded to the Anonymous Referee #1, we are so sorry for the incorrectly expression “long transports from Yellow Sea, East Sea, and South Sea were also important potential sources for NO_x and O₃” in the initial manuscript. After careful examination, we found that air masses with the seemed high WPSCF values for NO_x were not originating far from these open seas. They were just the broadening “tails” of high values contained in the areas with intensive anthropogenic NO_x emissions from inland well-industrialized cities. This phenomenon was also found in other studies by using trajectory statistical method (Riuttanen et al., 2013).

Similar with NO_x , air masses containing the high WPSCF values of O_3 also didn't come from the open seas. Indeed, such air masses were mostly from the offshore area of East China Sea, Yellow China Sea, or South China, respectively on southeastern Zhejiang, Jiangsu, and Fujian Province. We speculated the recirculation of pollutants by sea- and land-breeze circulations around the cities along the YRD and Hangzhou Bay which has been confirmed by Li et al. (2015, 2016b), was largely responsible for the increased concentration of O_3 at NRCS site. Also, such an increase in O_3 concentrations in urbanized coastal areas have been observed and modeled in a number of studies (Oh et al., 2006; Levy et al., 2008; Martins et al., 2012). Moreover, to further judge whether air masses came from open seas contained higher concentrations of NO_x and O_3 , we used the results of MOZART-4/GEOS-5 simulation to draw the distribution maps of NO_x and O_3 concentrations within the identical domain (15-55 °N and 105-135 °E) with WPSCF analysis. As clearly seen from the Figure 2 below, high NO_x mainly distributed in terrestrial regions, especially in industrialized cities, but very low NO_x were found in open seas. In comparison, significantly high O_3 were elucidated covering the offshore regions of either East China Sea, Yellow China Sea, or South China (Fig. 1). Then, along with the seasonal cluster analysis of back trajectories from NRCS site in Hangzhou, it's well confirmed that our speculation about the contribution of the recirculation of pollutants by sea- and land-breeze circulations in the offshore area to the observed O_3 at NRCS site.

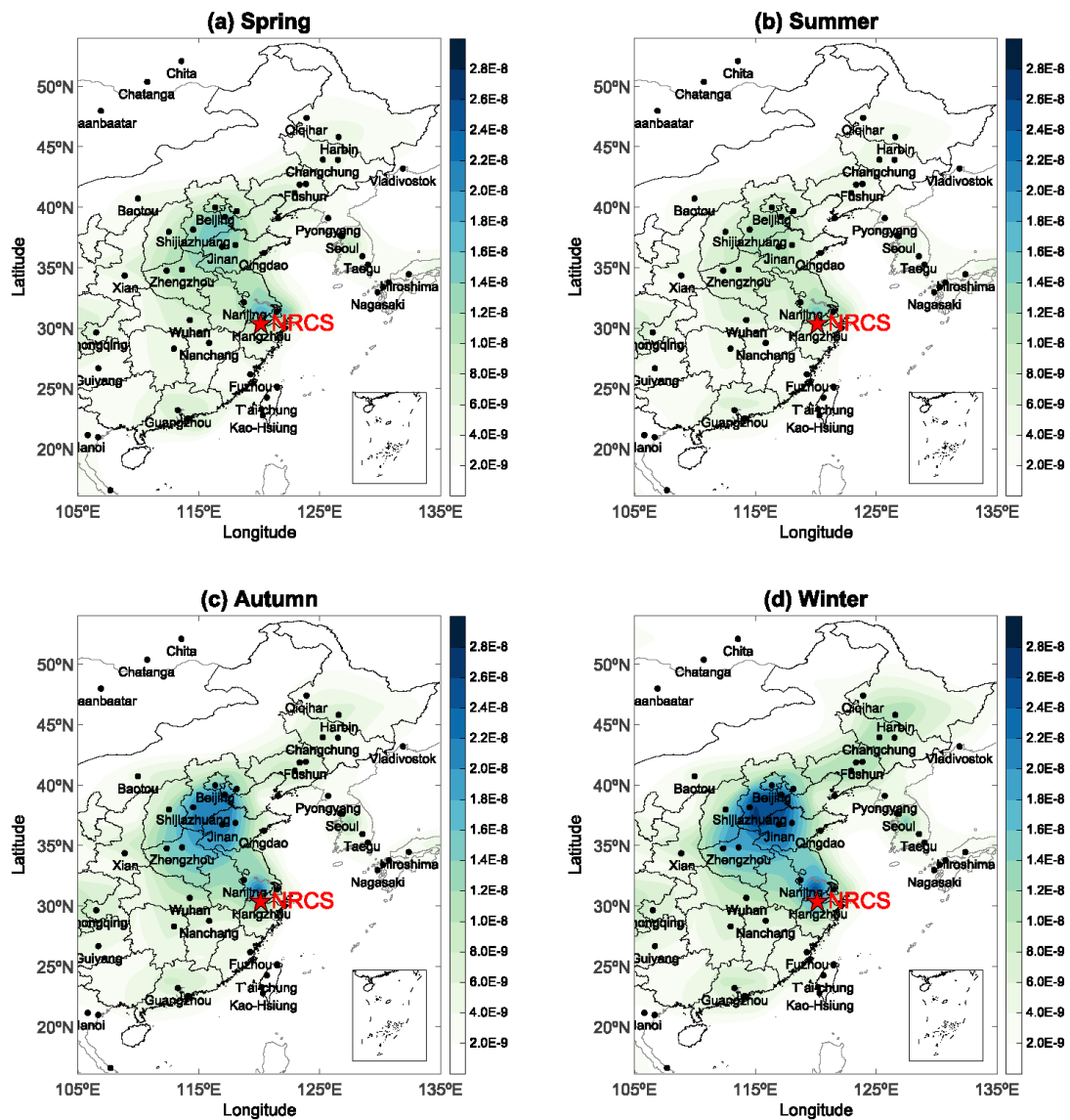


Figure 2 Seasonal and spatial distributions of NO_x volume mixing ratio (VMR) simulated by MOZART-4/GEOS-5. The sample site is marked in pentacle.

In summary, we made the corresponding corrections in the revised manuscript.

References:

- Brankov, E., Henry, R.F., Civverlo, K.L., Hao, W., Rao, S.T., Misra, P.K., Bloxam, R., and Reid, N.: Assessing the effects of transboundary ozone pollution between Ontario, Canada and New York, USA, *Environ. Pollut.*, 123, 403-411, 2003.
- Dickerson, R. R., Doddridge, B. G., and Kelley, P.: Large-scale pollution of the atmosphere over the remote Atlantic Ocean: Evidence from Bermuda, *J. Geophys. Res.*, 100, 8945-8952, 1995.
- Johnson, D., Mignacca, D., Herod, D., Jutzi, D., and Miller, H.: Characterization of identification of trends in average ambient ozone and fine particulate matter levels through trajectory cluster analysis in eastern Canada, *57(8)*, 907-918, 2007.
- Kaiser, A., Scheifinger, H., Spangl, W. G., Weiss, A., Gilge, S., Fricke, W. G., Ries, L., Cemas, D., and

Jesenovec, B.: Transport of nitrogen oxides, carbon monoxide and ozone to the Alpine global atmospheric watch stations Jungfrauoch (Switzerland), Zugspitze and Hohenpeissenberg (Germany), Sonnblick (Austria) and Mt. Krvavec (Slovenia), *Atmos. Environ.*, 41, 9273-9287, 2007.

Poirot, R. L. and Wishinski, P. R.: Long-term ozone trajectory climatology for the eastern US, 2, Results, 98-TP43.06 (A615), paper presented at the 91st Air and Water Management Association Annual Meeting and Exhibition, San Diego, Calif., 14-18 June, 1998.

Riccio, A., Giunta, G., and Chianese, E.: The application of a trajectory classification procedure to interpret air pollution measurements in the urban area of Naples (Southern Italy), *Sci. Total. Environ.*, 376, 198-214, 2007.

Riuttanen, L., Hulkkonen, M., Dal Maso, M., Junninen, H., and Kulmala, M.: Trajectory analysis of atmospheric transport of fine particles, SO₂, NO_x and O₃ to the SMEAR II station in Finland in 1996-2008, *Atmos. Chem. Phys.*, 13, 2153-2164, 2013.

Schlink, U., Dorling, S., Pelikan, E., Nunnari, G., Cawley, G., Junninen, H., Greig, A., Foxall, R., Eben, K., Chatterton, T., Vondracek, J., Richter, M., Dostal, M., Bertuccio, L., Kolehmainen, M., and Doyle, M.: A rigorous inter-comparison of ground-level ozone predictions, *Atmos. Environ.*, 37(23), 3237-3253, 2003.

Sharma, A., Mandal, T. K., Sharma, S. K., Shukla, D. K., and Singh, S.: Relationship of surface ozone with its precursors, particulate matter and meteorology over Delhi, *J. Atmos. Chem.*, 74(4), 451-474, 2017.

Siroris, A. and Bottenheim, J. W.: Use of backward trajectories to interpret the 5-year record of PAN and O₃ ambient air concentrations at Kejimikujik National Park, Nova Scotia, *J. Geophys. Res.*, 100, 2867-2881, 1995.

Stohl, A. and Kromp-Kolb, H.: Origin of ozone in Vienna and surroundings, Austria, *Atmos. Environ.*, 28, 1255-1266, 1994

Vellingiri K., Kim, K. H., Lim, J. M., Lee, J. H., Ma, C. J., Jeon, B. H., Sohn, J. R., Kumar, P., and Kang, C. H.: Identification of nitrogen dioxide and ozone source regions for an urban area in Korea using back trajectory analysis, *Atmos. Res.*, 176-177, 212-221, 2016.

Wu, J., Xu, C., Wang, Q. Z., and Cheng, W.: Potential sources and formations of the PM_{2.5} pollution in urban Hangzhou, *Atmosphere*, 7(100), 1-15, 2016.

Yu, S. C., Zhang, Q. Y., Yan, R. C., Wang, S., Li, P. F., Chen, B. X., Liu, W. P., and Zhang, X. Y.: Origin of air pollution during a weekly heavy haze episode in Hangzhou, China, *Environ. Chem. Lett.*, 12, 543-550, 2014.

1 **Characterization of atmospheric trace gases and particulate matters** 2 **in Hangzhou, China**

3 Gen Zhang¹, Honghui Xu², Bing Qi³, Rongguang Du³, Ke Gui¹, Hongli Wang⁴, Wanting Jiang⁵, Linlin
4 Liang¹, Wanyun Xu¹

5 ¹State Key Laboratory of Severe Weather & Key Laboratory of Atmospheric Chemistry of CMA, Chinese Academy of
6 Meteorological Sciences, Beijing 100081, China

7 ²Zhejiang Institute of Meteorological Science, Hangzhou 310008, China

8 ³Hangzhou Meteorological Bureau, Hangzhou 310051, China

9 ⁴State Environmental Protection Key Laboratory of Formation and Prevention of Urban Air Pollution Complex, Shanghai
10 Academy of Environmental Sciences, Shanghai 200233, China

11 ⁵Plateau Atmospheric and Environment Laboratory of Sichuan Province, College of Atmospheric Science, Chengdu
12 University of Information Technology, Chengdu 610225, China

13 *Correspondence to:* Gen Zhang (zhanggen@cma.gov.cn) and Honghui Xu (forsnow@126.com)

14 **Abstract.** The Yangtze River Delta (YRD) is one of the most densely populated regions in China with severe air quality
15 issues, which has not been fully understood. Thus, in this study, based on one-year (2013) continuous measurement at a
16 National Reference Climatological Station (NRCS, 30.22°N, 120.17°E, 41.7 m a. s. l) in the center of Hangzhou in the YRD,
17 we investigated the seasonal characteristics, interspecies relationships, and the local emissions and the regional potential
18 source contributions of trace gases (including O₃, NO_x, NO_y, SO₂ and CO) and particulate matters (PM_{2.5} and PM₁₀). Results
19 revealed severe two-tier air pollution (photochemical and haze pollution) occurred in this region, with frequent exceedances
20 in O₃ (38 days) and PM_{2.5} (62 days). O₃ and PM_{2.5} both exhibited distinct seasonal variations with reversed patterns: O₃
21 reaching a maximum in warm seasons (May and July) but PM_{2.5} in cold seasons (November to January). The overall results
22 from interspecies correlation indicated a strong local photochemistry favoring the O₃ production under a volatile organic
23 compound (VOC)-limited regime, whereas it moved towards an optimum O₃ production zone during warm seasons,
24 accompanying with a formation of secondary fine particulates under high O₃. The emission maps of PM_{2.5}, CO, NO_x, and
25 SO₂ demonstrated that local emissions were both significant for these species on seasonal scale. The contributions from the
26 regional transports among inland cities (Zhejiang, Jiangsu, Anhui, and Jiangxi Province) on seasonal scale were further
27 confirmed to be crucial to air pollution at NRCS site by using the backward trajectories simulations. Air masses transported,
28 from the offshore area of Yellow Sea, East Sea, and South Sea were also found to be highly relevant to the elevated O₃ at
29 NRCS site through the analysis of potential source contribution function (PSCF). Case studies of photochemical pollution
30 (O₃) and haze (PM_{2.5}) episodes both suggested the combined importance of local atmospheric photochemistry and synoptic
31 conditions during the accumulation (related with anticyclones) and dilution process (related with cyclones). Apart from

删除的内容: particle

删除的内容: zhangg@camsma

删除的内容: particles

删除的内容:

删除的内容: pollutants, especially for NO_x and O₃.

删除的内容: This study supplements

39 | supplementing a general picture of the air pollution state in urban Hangzhou in the YRD region, this study specifically
40 | elucidates the role of local emission and regional transport, and interprets the physical and photochemical processes during
41 | haze and photochemical pollution episodes. Moreover, this work suggests that cross-regional control measures are crucial to
42 | improve air quality in the YRD region, and further emphasizes the importance of local thermally induced circulation on air
43 | quality.

44 | 1 Introduction

45 | Ambient air quality is mainly affected by particulate matters (PM_{2.5} and PM₁₀) and gaseous pollutants such as ozone (O₃),
46 | nitrogen oxides (NO_x), carbon monoxide (CO), and sulfur dioxide (SO₂). Particulate matters are both from natural sources
47 | (e.g., windborne dust, volcanoes) or anthropogenic activities such as fossil and biomass fuel combustion (Chow and Watson,
48 | 2002). In addition to the net downward transport of O₃ by eddy diffusion from the stratosphere aloft, tropospheric O₃ is a
49 | well-known secondary gaseous pollutant and formed through the photochemical oxidation of volatile organic compounds
50 | (VOCs) and NO_x under the irradiation of sunlight (Logan, 1985; Roelofs et al., 1997). These chemicals both have received
51 | extensive attention either due to their harmful impact on human health (Pope et al., 1999; Shao et al., 2006; Streets et al.,
52 | 2007; Liu et al., 2013) and vegetation (Feng et al., 2014) or significant effects on climate change (Seinfeld et al., 2004; IPCC,
53 | 2007; Mercado et al., 2009). Moreover, some critical interactions have been verified existing between the gaseous pollutants
54 | and/or particulate matters (Zhang et al., 2004; Cheng et al., 2016). For instance, in the presence of high NH₃ and low air
55 | temperature, ammonium nitrate (NH₄NO₃) is formed in regions with HNO₃ and NH₃, which is an important constituent of
56 | PM_{2.5} under the high NO_x condition (Seinfeld and Pandis, 2006). To some extent, such interactions further improve or
57 | deteriorate the air quality. The oxidation of SO₂ leads to acid deposition but also contributes to the formation of sulphate
58 | aerosols (Meagher et al., 1978; Saxena and Seigneur, 1987), which in turn will influence the solar radiation and
59 | photochemistry (Dickerson et al., 1997) and further weaken the formation of secondary pollutants. Therefore, clear
60 | understanding in their characteristics, sources, transport, and formation mechanisms including interactions is crucial for
61 | gaining the comprehensive information on the complex air pollution.

62 | The Yangtze River Delta (YRD) region is located in the eastern of China, including the mega-city Shanghai and the well-
63 | industrialized areas of southern Jiangsu Province and northern Zhejiang Province, with over ten large cities such as
64 | Hangzhou, Suzhou, Wuxi and Changzhou lying along the mid-YRD (Fig. 1). Being one of the most rapid growths of
65 | transportation, industries, and urbanization regions in China, it has been became hot spot with air pollution over the past
66 | three decades, together with the Pearl River Delta (PRD) and Beijing-Tianjin-Hebei (BTH) region. To date, numerous
67 | combined studies of O₃ and PM_{2.5} were implemented in representative urban cities in YRD region such as Shanghai (Geng et
68 | al., 2007; Ding et al., 2013; Li et al., 2016a; Miao et al., 2017a) and Nanjing (Wang et al., 2002; Wang et al., 2003; Kang et
69 | al., 2013; Chen et al., 2016). On the contrary, in Hangzhou (29.25°-30.5°N, 118.34°-120.75°E), a capital city of Zhejiang
70 | Province in YRD region, which is lying along the mid-YRD, only a few sole studies of PM_{2.5} or O₃ were sporadically
71 | conducted. PM_{2.5} measurements in urban Hangzhou have been performed only in the past five years, mostly covering short-

删除的内容: particle

删除的内容: Particle

删除的内容: (PM_{2.5} and PM₁₀)

删除的内容: They have received extensive attention due to their harmful impact not only on human health such as aggravating chronic respiratory and cardiovascular diseases (Pope et al., 1999) but also

已下移 [1]: on climate change (Seinfeld et al., 2004; IPCC, 2007; Mercado et al., 2009)

删除的内容:). As primary gaseous pollutants, NO_x, CO, and SO₂ are all trace gases and derived from the anthropogenic activities (Kato and Akimoto, 1994; Streets and Waldhoff, 2000). NO_x, with a short lifetime, is mainly emitted from the fuel burning in the polluted region. In contrast, CO has a relatively long atmospheric lifetime and emitted from the combustion sources, thus it's also a preferred tracer for indicating the anthropogenic pollution and charactering the other pollutants (Jaffe et al., 1997; Parrish et al., 1998).

删除的内容: pollutants

删除的内容: nitrogen oxides (

删除的内容:)

删除的内容:), which has been also increasingly concerned with its adverse effect

删除的内容: exacerbating chronic respiratory diseases and causing short-term reductions in lung function (

已移动(插入) [1]

删除的内容:). Reactive nitrogen (NO_y) is defined as the sum of NO_x and all compounds that are products of the atmospheric oxidation of NO_x (e.g., PANs, HNO₃, and HONO). Except NO_x, the other constituents in NO_y are also mainly produced via the complex conversions within primary gaseous pollutants (i.e., photochemical oxidation and nighttime chemistry

删除的内容:

删除的内容: particle

删除的内容: can lead

删除的内容: problems

119 term period in winter (Jansen et al., 2014; Yu et al., 2014; Liu et al., 2015; Wu et al., 2016). Furthermore, there was still
120 certain discrepancy about the origin of PM_{2.5}. Wu et al. (2016a) concluded that the local vehicle emission was a major
121 contribution to PM_{2.5}, while results from Yu et al. (2014) suggested cross-border transports rather than local emissions
122 control high PM_{2.5} concentration and formation. Similarly, the photochemical pollution in urban Hangzhou was also not well
123 understood. To our knowledge, the pioneer measurement of O₃ in or around Hangzhou started in the 1990s at Lin'an site, a
124 regional station located in the eastern Zhejiang Province (50 km away from Hangzhou) (Luo et al., 2000). Subsequent
125 studies at this site depicted the first picture of the seasonal variations of O₃ and its precursors (Wang et al., 2001; Wang et al.,
126 2004). In urban Hangzhou, only short-term measurements of O₃ were recently made during the summertime of 2013, (Li et
127 al., 2017). Hence, there are large knowledge gap on seasonal characteristics of these pollutants and discrepancy on their
128 origin, which are both crucial for fully understanding the complex combined pollution of PM_{2.5} and O₃ in urban Hangzhou.

129 To supplement the seasonal picture of air pollution in YRD, we conducted continuous measurements of trace gases (O₃,
130 NO_x, NO_y, CO, and SO₂) and particulate matters (PM_{2.5} and PM₁₀) during January-December 2013 at a regional site NRCS
131 (National Reference Climatological Station) in Hangzhou, which is also an integrated measurement site for the research of
132 climate change and atmospheric environment. This study presents the first results of one-year measurements of trace gases
133 and particulate matters in urban Hangzhou, investigates the characteristics and cause of these chemicals by discussing their
134 seasonal characteristics, interspecies correlations, the concentration dependence on local emission and regional transport, and
135 the specific photochemical pollution and haze case, respectively.

136 **2 Experiment and meteorological conditions,**

137 **2.1 Site description**

138 Hangzhou is situated in the eastern coast of China and is one of the most developed cities in the Yangtze River Delta region.
139 It has 8.9 million population and 2.7 million vehicles according to the 2014 Statistical Bulletin of Hangzhou. It belongs to
140 the subtropical monsoon climate, with an average temperature of 17.0°C, relative humidity of 75% and rainfall of 1438 mm
141 over the past 30 years (1981-2010). In this study, all in-situ measurements of gaseous constituents, particulates and
142 meteorological factors were conducted at a site named NRCS (30.22°N, 120.17°E, 41.7 m a.s.l) in the center of Hangzhou
143 (Fig. 1). As a typical urban site, NRCS station is situated in the commercial and residential areas in the southern Hangzhou
144 and thus it's characterized as a polluted receptor site as it receives local urban plumes and regional air masses from the YRD
145 region when northwesterly wind prevails. Moreover, as the right top map shown in Fig. 1, the site is adjacent to Prince Bay
146 Park (area, 0.8 km²) and situated in the northeastern part of West Lake famous scenic spot (area, 49 km²). Therefore it can
147 also capture the signature of vegetation emission in urban Hangzhou under southwesterly winds. Moreover, there are no
148 local industrial pollution sources around the site. In brief, this site can be representative of urban Hangzhou.

删除的内容: east

删除的内容: Xu et al. (2016) concluded the medium long range boundary transport of air masses coming from biomass burning regions was responsible for the formation of haze aerosols at Lin'an site during the winter.

删除的内容: the

删除的内容: Li et al (2017) recently reported the results of

删除的内容: , CO, and non-methane hydrocarbons at three sites in Hangzhou in the

删除的内容: In terms of particle matters, Wu et al. (2016a) reported that the local vehicle emission was a major contribution to PM_{2.5}, while results from Yu et al. (2014) suggested cross-border transports rather than local emissions control high PM_{2.5} concentration and formation.

删除的内容: still exist in

删除的内容: and PM_{2.5}

删除的内容: the

删除的内容: particle

删除的内容: particle

删除的内容: the

删除的内容: area of

删除的内容: Introduction to the experiment,

删除的内容: , and methodology

带格式的: 到齐到网格

删除的内容: particles

删除的内容: NRCS

删除的内容:) and commercial and residential areas in

删除的内容: south

删除的内容: city. There

删除的内容: Thus, all gaseous constituents at

删除的内容: the

删除的内容: areas in

带格式的: 字体: 加粗

190 2.2 Measurements description

191 Measurements of trace gases, aerosols, and meteorological parameters were conducted at NRCS station during January-
192 December 2013. Trace gases including O₃ and SO₂ were detected by a set of commercial trace gas analyzers (Thermo
193 Environmental Instruments Inc., USA i-series 49i, 43i), respectively, with a resolution of 1 min. NO and NO_x were detected
194 by a chemiluminescence analyzer coupled with an internal MoO catalytic converter (TEI, 42i). Note that the differentiated
195 value of NO₂ from NO_x and NO represents the upper limit concentration of atmospheric NO₂ due to the interference of other
196 nitrogen-containing components (e.g., PAN, HNO₃, and HONO) in the conversion. Similar with NO_x, NO_y was also detected
197 by a chemiluminescence analyzer (TEI 42i-Y) but equipped with an external MoO catalytic converter. CO was monitored
198 with a gas filter correlation, infrared absorption analyser (TEI, 48i), with automatic zeroing every 6 hours. All the
199 instruments are housed on the top floor of a laboratory building, which sits on the top of a hill about 40 m above the ground
200 level. Ambient air was drawn from the 1.5 m above the rooftop to the laboratory building through a manifold connected to
201 O₃, SO₂, NO and CO analyzers with PFA Teflon tubes (inside diameter: 2 cm). A separate sample line with a MoO converter
202 was used for NO_y analyzer. All trace gas analyzers were weekly span and daily zero checked, except CO, and multi-point
203 calibration was made once a month.

204 Ambient PM_{2.5} samples were collected using co-located Thermo Scientific (formerly R&P) Model 1405D samplers. The
205 sensor unit contains the two mass measurement hardware systems that monitor particulates that continuously accumulate on
206 the system's exchangeable TEOM filters. PM-Coarse and PM_{2.5} particulate, split by a virtual impactor, each accumulate on
207 the system's exchangeable TEOM filters. By maintaining a flow rate of 1.67 L·min⁻¹ through the coarse sample flow channel
208 and 3 L·min⁻¹ through the PM_{2.5} sample channel, and measuring the total mass accumulated on each of the TEOM filters, the
209 device can calculate the mass concentration of both the PM_{2.5} and PM Coarse sample streams in near real-time. TEOM filters
210 must be replaced before the filter loading percentage reaches 80% to ensure the quality of the data generated by the
211 instrument. For PM, the precisions of this instrument were 2.0 µg cm⁻³ for 1 h average and 1.0 µg cm⁻³ for 24 h average.

212 2.3 Meteorological characteristic

213 Table 1 shows the monthly averaged meteorological parameters at NRCS station, suggesting distinct characteristics of air
214 temperature in winter and summer in this region, with monthly averages from ca. 5 °C in January to ca. 32 °C in July. High
215 relative humidity (RH) and a large amount of rainfall appeared in June (346 mm in total), and oppositely less precipitation
216 and low RH in autumn and winter. Note that the seemed high RH and large rainfall occurred in October was due to an
217 extremely synoptic event on 7 October, 2013 with the daily total rainfall of 91 mm. In addition, the wind rose implied that
218 the prevailing wind was from northwest in autumn, north in winter, and from southwest in spring and summer (See Fig. S1
219 in the Supplement).

220 ▲

带格式的：定义网格后不调整右缩进，不调整西文与中文之间的空格，不调整中文和数字之间的空格，不对齐到网格

删除的内容：, SO₂, NO, NO_x,

删除的内容：CO

删除的内容：, 42i, 42i-Y, and 48i), respectively, with a resolution of 1 min.

删除的内容：particles

带格式的：字体：加粗

226 **2.4 Methodology**

227 **2.4.1 Air mass back trajectory cluster**

228 In this study, 72-h back trajectories starting at the arrival level of 100 m from NRCS sites were calculated by using the
 229 National Oceanic and Atmospheric Administration (NOAA) HYSPLIT-4 model with a $1^\circ \times 1^\circ$ grid and the final
 230 meteorological database. The six hourly final archive data were obtained from the National Center for Environmental
 231 Prediction's Global Data Assimilation System (GDAS) wind field reanalysis. GDAS uses a spectral medium-range forecast
 232 model. More details could be found at <http://www.arl.noaa.gov/ready/open/hysplit4.html>. The model was run four times per
 233 day at starting times of 00:00, 6:00, 12:00, and 18:00 UTC (08:00, 14:00, 20:00, and 02:00 LT, respectively). The method
 234 used in trajectory clustering was based on the GIS-based software TrajStat (Wang et al. 2004).

235 **2.4.2 Potential source contribution function**

236 The potential source contribution function (PSCF) is widely used to identify regional sources based on the HYSPLIT model.
 237 The zone of concern is divided into $i \times j$ small equal grid cells. The PSCF value in the ij -th cell is defined as m_{ij}/n_{ij} , where n_{ij}
 238 is denoted as the numbers of endpoints that fall in the ij -th cell and m_{ij} represents the numbers of "polluted" trajectory
 239 endpoints in the ij -th cell. In this analysis, average concentrations were considered as the "polluted" threshold (Hsu et al.,
 240 2003; Zhang et al., 2013). To minimize the effect of small values of n_{ij} , following the method of Polissar et al. (1999), the
 241 seasonal PSCF values were multiplied by arbitrary seasonal weight functions W_{ij} , expressed by WPSCF, to better reflect the
 242 uncertainty in the values for these cells. Geographic areas covered by more than 95% of the back trajectories are selected as
 243 the study domain. In this study, our study domain was in the range of $15\text{-}55^\circ\text{N}$ and $105\text{-}135^\circ\text{E}$. The resolution was $0.5^\circ \times 0.5^\circ$.

244

$$W_{ij(\text{spring})} = \begin{cases} 1.00 & 36 < n_{ij} \\ 0.70 & 12 < n_{ij} \leq 36 \\ 0.42 & 6 < n_{ij} \leq 12 \\ 0.17 & n_{ij} \leq 6 \end{cases} - W_{ij(\text{summer})} = \begin{cases} 1.00 & 42 < n_{ij} \\ 0.70 & 14 < n_{ij} \leq 42 \\ 0.42 & 7 < n_{ij} \leq 14 \\ 0.17 & n_{ij} \leq 7 \end{cases}$$

245

$$W_{ij(\text{autumn})} = \begin{cases} 1.00 & 36 < n_{ij} \\ 0.70 & 12 < n_{ij} \leq 36 \\ 0.42 & 6 < n_{ij} \leq 12 \\ 0.17 & n_{ij} \leq 6 \end{cases} - W_{ij(\text{winter})} = \begin{cases} 1.00 & 54 < n_{ij} \\ 0.70 & 18 < n_{ij} \leq 54 \\ 0.42 & 9 < n_{ij} \leq 18 \\ 0.17 & n_{ij} \leq 9 \end{cases}$$

246 Moreover, to better elucidate the local and regional contribution to pollutants concentrations, we further compared the
 247 WPSCF results with their corresponding emission inventories of $\text{PM}_{2.5}$, CO , NO_x , and SO_2 in 2013 provided by Peking
 248 University (<http://inventory.pku.edu.cn/>), which were estimated by using a bottom-up approach with $0.1^\circ \times 0.1^\circ$ spatial
 249 resolution (Wang et al., 2013; Huang et al., 2014; Zhong et al., 2014), respectively.

删除的内容: showed

$$\text{删除的内容: } W_{ij(\text{spring})} = \begin{cases} 1.00 \\ 0.70 \\ 0.42 \\ 0.17 \end{cases}$$

$$\left. \begin{matrix} 36 < n_{ij} \\ 12 < n_{ij} \leq 36 \\ 6 < n_{ij} \leq 12 \\ n_{ij} \leq 6 \end{matrix} \right\}$$

$$W_{ij(\text{summer})} = \begin{cases} 1.00 \\ 0.70 \\ 0.42 \\ 0.17 \end{cases}$$

$$\left. \begin{matrix} 42 < n_{ij} \\ 14 < n_{ij} \leq 42 \\ 7 < n_{ij} \leq 14 \\ n_{ij} \leq 7 \end{matrix} \right\}$$

$$W_{ij(\text{autumn})} = \begin{cases} 1.00 \\ 0.70 \\ 0.42 \\ 0.17 \end{cases}$$

$$\left. \begin{matrix} 36 < n_{ij} \\ 12 < n_{ij} \leq 36 \\ 6 < n_{ij} \leq 12 \\ n_{ij} \leq 6 \end{matrix} \right\}$$

265 2.4.3 Geopotential height (GH)

266 The geopotential height (GH) fields derived from the National Center for Environmental Prediction (NCEP) global Final
267 (FNL) reanalysis (<http://rda.ucar.edu/datasets/ds083.2/>) are typically used to classify the synoptic types (Miao et al., 2017b).
268 In this study, daily GH fields at the 925 hPa level from the NCEP-FNL reanalysis covering the region (100-135 °E, 20-50 °N)
269 were classified to the prevailing synoptic types during photochemical pollution and haze episodes as discussed in Section 3.5.
270 The NECP-FNL reanalysis was produced from the Global Data Assimilation System, which continuously assimilates
271 observations from the Global Telecommunication System and other sources. The NECP-FNL reanalysis fields were on $1^{\circ} \times 1^{\circ}$
272 grids with a 6 h resolution.

273 3 Results and discussion

274 3.1 Concentration levels

275 To evaluate the overall concentration level of gaseous and **particulate** pollution at NRCS, we selected a Grade II standard of
276 the Chinese Ambient Air Quality Standards (CAAQS, GB 3095-2012), which was released in 2012 by the China State
277 Council and implemented thorough the whole nation in 2016 (MEP, 2012). Inferred from the Grade II CAAQS for $PM_{2.5}$ (75
278 $\mu g m^{-3}$ for 24 h average) and PM_{10} (150 $\mu g m^{-3}$ for 24 h average), 62 days and 26 days of $PM_{2.5}$ and PM_{10} exceedances with
279 daily average of 102.2 $\mu g m^{-3}$ and 195.3 $\mu g m^{-3}$ were classified thorough the period, respectively, mostly occurred in winter.

280 For O_3 , about 38 days exceedances (75 ppbv for **daily maximum 8 h** average for the Grade II CAAQS) in whole were found
281 during the whole period, mostly covering from May to September. It suggested Hangzhou was suffering from heavy haze
282 and photochemical pollution in cold and warm seasons. Concerning SO_2 , the annual mean was 10.9 ppbv in this study,
283 nearly half of the yearly mean of SO_2 Grade II CAAQS (21 ppbv). It was reasonably attributed to the powerful measure of
284 Chinese government to control the emission of SO_2 starting at 1990 (He et al., 2002; Qi et al., 2012). Table 2 summarized a
285 statistical analysis on these species and listed the comparison with the previous results in other typical regions in China. In
286 general, with respect to all these chemicals, our results were generally comparable with those observed by other

287 contemporaneous measurements in Hangzhou and the other cities in YRD. As expected, regional differences **among** YRD,
288 PRD, and BTH could be also found as illustrated in Table 2. For instance, observed $PM_{2.5}$, PM_{10} , and CO concentrations
289 were higher in BTH than those in YRD and PRD through the comparison among provincial capital cities in China during
290 2011-2014 (Chai et al., 2014; Wang et al., 2014), which has been extrapolated to be more emissions from coal-based
291 industries and coal and biomass burning based domestic home heating in BTH in winter (Zhang et al., 2012; Yang et al.,
292 2013; Chai et al., 2014). Moreover, slight decreases in $PM_{2.5}$ and PM_{10} at NRCS were both evidenced by their respective
293 difference between 2013 and 2010-2011 (Tab. 2), coincident with the results derived from the satellite data and ground
294 monitoring in China (Ma et al., 2016; Seltnerich, 2016). For NO_y , only rough comparison was implemented due to very
295 limited measurements executed in China. The yearly mean NO_y concentration of 63.7 ppbv in this study was slightly higher
296 than 54.6 ppbv in Beijing (Wu et al., 2016b). It's interestingly noted that slightly higher NO_y at NRCS possibly indicated

删除的内容: particle

删除的内容: 93

删除的内容: 1

删除的内容: between

301 | more abundance of nitrogen oxides in Hangzhou. Additionally, the daytime mean concentrations were comparable with
302 | those at nighttime for PM_{2.5} nearly in all seasons but higher for O₃ due to the daily variations in solar radiation and air
303 | temperature, the reverse is true for CO, NO_x, and NO_y.

删除的内容: photochemical conversion

删除的内容: NO_x

删除的内容: than Nanjing in the presence of nearly identical NO₂

304 3.2 Seasonal characteristics

305 | Figure 2 shows seasonal variations of atmospheric O₃ (a), CO (b), NO (c), NO_x (d), NO_y (e), O_x (f), PM_{2.5} (g), PM₁₀ (h), and
306 | SO₂ (i). Ozone exhibits a distinguished seasonal variation, with a board peak in late spring and middle summer (a maximum
307 | in May and a secondary maximum in July) and a minimum in winter (November to January). Its observed behavior at NRCS
308 | is different from what has been disclosed in previous studies conducted in southern and northern China, such as a summer
309 | minimum and an autumn maximum of O₃ found in Hong Kong and an early summer (June) broad maximum recorded in
310 | Beijing (Ding et al., 2008; Lin et al., 2008, 2009; Xue et al., 2014; Zhang et al., 2014; Sun et al., 2016). Recently, Ding et al.
311 | (2013) presented two peaks of O₃ appearing in summer (July) and early autumn (September) at Xianlin site in the suburban
312 | area northeast of Nanjing (about 239 km away from NRCS station). Regarding the geographical location of Hangzhou,
313 | which is upwind of the YRD under the influence of southeasterly summer monsoon, the emissions in the YRD region and
314 | the solar radiation might be the main causes of an O₃ formation in summer, resulting in a different seasonal cycle of O₃
315 | compared to other continent sites in the west/northwest YRD. In fact, the CO and NO_y data (Fig. 2b and Fig. 2e) show that
316 | these precursors were still at fairly high levels (about 500 ppbv and 35 ppbv, respectively) in summer. The low O₃ level in
317 | winter, especially at night, can be attributed to the lower temperature, weaker solar radiation, and in particular the strong
318 | destruction of O₃ by chemical titration of NO from local emission or regional transport as discussed below (Lin et al., 2008,
319 | 2009, 2011). Note that, a slight drop of O₃ was found in June compared with other months in summer, mainly attributing to
320 | the more frequent rainy days (23 days) and larger rainfall in June (346 mm) than those in May (15 days) and July (5 days)
321 | during summertime (Table 1).

删除的内容: Xianlin

322 | For PM_{2.5} and PM₁₀, Fig. 2g and -2h both displayed overall well-defined seasonal variations with the maximum in winter
323 | (December) and the minimum in summer (July). In cold seasons the emission of particulate matter is normally high due to
324 | more emission of fossil fuels during heating in northern China (Zhang et al., 2009), which contributed to the enhancements
325 | of particulate matters and other tracer gases (i.e., CO and NO_x) at NRCS site via long-distance transport (See discussion in
326 | Section 3.4). Furthermore, in winter temperature inversion and low mixing layer contribute to decrease particulate
327 | suspension and advection (Miao et al., 2015a). Also, dry/wet deposition should have strong seasonal variations because high
328 | precipitation favors wet-deposition and high soil humidity, and the growth of deciduous plants may also favor the dry
329 | deposition of particulate matter in warm seasons (Zhang et al., 2001). The relatively low concentrations of PM_{2.5} and PM₁₀ in
330 | summer may be also partly due to an increased vertical mixing (i.e., a higher boundary layer height) and more convection
331 | (Ding et al., 2013; Miao et al., 2015b). PM_{2.5} mass concentration also show strong month-to-month variations. The
332 | simultaneous drop of PM_{2.5} and PM₁₀ concentrations together with other primary pollutants (i.e., SO₂, CO and NO_y) in
333 | February was mainly ascribed to the winter break of the Chinese Spring Festival, which started at the end of January and

删除的内容: particle

删除的内容: particle

删除的内容: particle

342 lasted until mid-February. Notably, the seasonal pattern for PM was similar to NO_x , which suggested that traffic and heating
343 emissions were important to the $\text{PM}_{2.5}$ variation.

344 For other trace gases (CO , NO_x , NO_y , and SO_2), they all revealed clear seasonal variations but also some unique month-to-
345 month variation patterns (Fig. 2a-2f and Fig. 2i). Similar seasonal patterns among CO , NO_x , and SO_2 were generally found
346 with pronounced minimums appearing in summer and higher levels in fall and winter. Similar reasons with particulate
347 matters could interpret these seasonal patterns such as the variation in the boundary layer height and the long-distance
348 transport as mentioned above. The last but not the least was photochemistry. During summer, it's most active to accelerate
349 the transformation of primary gaseous pollutants, whereas in winter, weaker photochemical reaction cannot remove the gases
350 as quickly as in the warmer seasons from the atmosphere.

351 NO_y concentration increased at the end of autumn, with a maximum in December together with a sharp peak of NO . Time
352 series implied that in December there was a multi-day episode of NO_x with high mixing ratios of NO and NO_2 both reaching
353 up to 100 ppbv and these days were generally correlated with northwest wind, suggesting a fresh emission from factories in
354 the industrial zone in the northwest. The "potential ozone" O_x ($\text{O}_3 + \text{NO}_2$) is usually used as an estimate of atmospheric total
355 oxidant (Lin et al., 2008). In summer (Fig. 2f), an abnormally high level of O_x was found in winter with low O_3 . The high
356 level of NO_2 in O_x was expected to be originated from the significant titration of high NO by O_3 in November and December
357 (Fig. 2a).

358 As shown in Fig. 2i, SO_2 displayed a strong increase in winter but a significant drop in November. This pronounced
359 winter peaks were mainly due to the increased coal consumption for heating as mentioned above. The drop was associated
360 with the $\text{PM}_{2.5}$ maximum and a relatively high RH (Fig. 2g and Table 1), suggesting a possible role of heterogeneous
361 reactions (Ravishankara, 1997).

362 3.3 Inter-species correlations

363 Inter-species correlation could be normally used as an agent for acquiring some insights on their chemical formation,
364 removal processes, and interactions. As displayed in Fig. 3 and Fig. 4, we presented scatter plots of NO_y - O_3 , NO_y - $\text{PM}_{2.5}$,
365 NO_y - SO_2 , O_3 - $\text{PM}_{2.5}$, and NO_y - CO correlations based on the whole dataset, respectively, and further discriminated these
366 correlations under typical environmental or meteorological impacts with color-coded parameters (i.e., relative humidity, air
367 temperature, and O_3 concentration). Clearly, overall negative correlation was found between O_3 and NO_y during the whole
368 period (Fig. 3a). The color data showed that negative correlation mainly appeared with data of low air temperature, implying
369 a remarkable titration of freshly emitted NO with O_3 during the cold seasons and at nighttime. In contrast, a positive
370 correlation between O_3 and NO_y dominated under high air temperature, which usually occurred in the daytime of warm
371 seasons within a moderate level of NO_y (<150 ppbv). These findings suggested a strong local photochemical production of
372 O_3 in summer, leading to its seasonal variations as illustrated in Fig. 2a.

373 As illustrated in Fig. 3b, a good positive correlation was found between $\text{PM}_{2.5}$ and NO_y , suggesting that $\text{PM}_{2.5}$ was highly
374 correlated with fossil combustion at this site. Some green data in the plot show very high NO_y concentration together with

删除的内容: particle

删除的内容: (mainly as NO_2)

删除的内容: but for

删除的内容: decreased

删除的内容: -7

删除的内容: O_3 -

删除的内容: .

删除的内容: -

删除的内容: .

删除的内容: $-\text{NO}_y$, $\text{CO}-\text{NO}_y$, and

删除的内容: $-\text{O}_3$

删除的内容: 3

删除的内容: 4

low PM_{2.5}, suggesting that high NO air masses during December. Fig. 3b exhibited that high RH data were very scattered but not very high PM_{2.5}/NO_y, implying that negligible interference of humidity on TEOM PM_{2.5} measurement during the study period, even under high RH condition in summer.

删除的内容: 4

SO₂ and NO_y show a moderate to good correlation (See Fig. 3c). Specifically, a better correlation and higher SO₂/NO_y ratio were gained from air with low humidity. Nevertheless, the point distribution was much more scattered for the humid air masses, and the ratio of SO₂/NO_y was clearly low, confirming a higher conversion of SO₂ to sulfate and/or deposition in the humid condition (Khoder, 2002; Su et al., 2011). In this study, the averaged ratios of SO₂/NO_y during 18 February-30 April was lower as 0.017, compared with that previously reported at Lin'an during the same months twelve years ago (Wang et al., 2004). It was mainly owing to a remarkable reduction of SO₂ emission from power plants but an increased NO_x emission associated with a huge consumption of petroleum fuels in the past decade in this region (Zhang et al., 2009).

删除的内容: 5

A scatter plot of O₃ with PM_{2.5} color-coded with air temperature was depicted in Fig. 3d. During moderate to high air temperature, a significant positive correlation was elucidated between O₃ and PM_{2.5} and the reverse negative correlation was found under low temperature. The positive correlation for warm air might reflect a formation of secondary fine particulates in summer associated with high O₃, which was confirmed by our comparison of the ratio of the averaged PM_{2.5} concentrations in the typical O₃ exceedances events (OE) to that in nearby non-O₃ exceedances (NOE) events (PM_{2.5}(OE)/PM_{2.5}(NOE)) with the ratios for other gaseous pollutants (Table S1 in the Supplement). The secondary particulate formation may be related to high conversion rate of SO₂ and NO_x to sulfate and nitrate under a high concentration of oxidants (Khoder, 2002; Sun et al., 2013). Additionally, it was also associated with the formation of secondary organic aerosols with high O₃ concentrations (Kamens et al., 1999; Lambe et al., 2015; Palm et al., 2017), which was primarily produced through the photo-oxidation of BVOCs (Claeys, et al., 2004; Böge et al., 2013). As inferred above, significant emission of BVOCs was speculated around NRCS in summer. Note that it's necessary to implement more detailed investigations related with chemical elements, ion, and OC/EC analysis of particulate matters. The anti-correlation for cold air might be caused by the titration effect of high NO concentration in relation to high primary PM_{2.5} in cold seasons, which was also reflected by the consistency of the seasonal variations in NO and PM_{2.5}.

已移动(插入) [2]

已移动(插入) [3]

已移动(插入) [4]

Figure 4 shows a good positive correlation between CO and NO_y color-coded with O₃ mixing ratios. For CO lower than 3.2 ppmv during the whole period, an increase of NO_y generally led to lower O₃ concentrations, but CO reversed. As a common origin of VOCs and CO, VOCs play a similar behavior with CO in the ozone photochemistry, in the typical urban region (Atkinson, 2000; Guo et al., 2004). Our results suggested a VOCs-limited regime throughout the year in Hangzhou, consistent with the reported results in other cities of YRD region (e.g., Shanghai and Nanjing) (Geng et al., 2007; Ding et al., 2013). While, as specifically shown in Fig. 4b, atmospheric O₃ (above 80 ppbv), mainly occurred in the afternoon (14:00-16:00 LT) in the summer and early autumn, exhibited increased trend with the increasing NO_y within air masses with moderated CO mixing ratio of 0.25-1.5 ppmv, and the reversed trend for CO was not expected to be significantly increased. It indicated that the transition from VOCs-limited regime to an optimum O₃ production zone (even NO_x-limited regime), probably occurred at NRCS site in warmer seasons. We speculated this change was mainly attributed to the larger emission

删除的内容: 6

删除的内容: leaded

删除的内容: .

删除的内容: 6b

428 of biogenic VOCs (BVOCs) compared to cold seasons. As reviewed by Calfapietra et al. (2013), the VOC-limited conditions,
429 in which O₃ production is limited by a high concentration of NO_x, are often observed in urban areas. However, if high
430 BVOC emitters are common in urban areas, they could move the VOC/NO_x ratio toward optimal values for O₃ formation,
431 and resulted in this ratio reaching in the city centers. As depicted in Section 2.1, our study site is situated adjacent to Prince
432 Bay Park (area, 0.8 km²) and in the northeast of West Lake famous scenic spot (area, 49 km²). For these two regions, they
433 were both block green parks with high vegetation coverage. Moreover, the primary tree species in these two regions are
434 Liquidambar formosana and Cinnamomum camphora, respectively, as major contributor to the emissions of isoprene and
435 monoterpene (Chang et al., 2012), favoring the formation of O₃. Air masses from Prince Bay Park and West Lake famous
436 scenic spot were confirmed to be transported to NRCS site during warmer seasons, as illustrated in Fig. S1 and Fig. 8b. In
437 view of the strong temperature dependence of isoprenoid emission (Guenther et al., 1995), a significantly increased emission
438 of BVOCs was expected in warm seasons and thus it disturbed the original balance between VOCs and NO_x relative to cold
439 seasons. Our conclusion was generally in line with the contemporaneous study implemented by Li et al. (2016a) who found
440 that VOCs-limited regime accounted for 47% of the ozone formation during the summer in Hangzhou, and the others are
441 under NO_x-limited, taking BVOCs into consideration. Recently, Li et al. (2017) also deduced the summer ozone mostly
442 presented VOCs-limited and transition region alternately in urban Hangzhou.

443 **3.4 Dependences of pollutant concentrations on local emission and regional transport**

444 To overview the impact of wind on the pollutants concentrations, we draw the seasonal wind dependence maps of pollutants
445 concentrations with wind sectors (See Fig. S2 in the Supplement for details). In total, similar seasonal patterns of wind
446 dependence map were found between CO and PM_{2.5}, SO₂, and NO_y (NO_x), in good agreement with their seasonal patterns as
447 shown in Section 3.2. For CO and PM_{2.5}, their top 10% concentrations were generally related with all the directions
448 throughout the year at speeds lower than 2 m s⁻¹ while bottom 10% were associated with others direction wind except north
449 at higher wind speed. It's necessary to pay attention to the scatter points of top 10% concentrations distributed in north
450 direction with high wind speed. With respect to the wind direction and transport, as the wind speed increases, pollutants
451 concentrations should have been decreasing due to the more effective local dilution, thus the increase instead might indicate
452 potential sources in these directions.

453 To address this issue and further investigate the relative contribution of local emission and regional transport, we
454 employed the trajectory clustering and WPSCF, along the comparison with the emission inventories. The 72 h back
455 trajectories from NRCS site were computed by using HYSPLIT model for four seasons. As shown in Fig. 9a, we obtained
456 six clusters by the clustering algorithm for four seasons with seven dominant paths distributed in east (E), northeast (NE),
457 north (N), northwest (NW), west (W), southwest (SW), and southeast (SE). The length of the cluster-mean trajectories
458 indicates the transport speed of air masses. In this analysis, the long and fast moving trajectories were disaggregated into
459 groups originating from more distant SE and SW regions during summer and NW and N regions during other seasons.
460 Member of this cluster have extremely long transport patterns, some of them even cross over Inner Mongolia and Mongolia

删除的内容: northeastern

删除的内容: addition to

已上移 [2]: A scatter plot of O₃ with PM_{2.5} color-coded with air temperature was depicted in Fig.

删除的内容: 7.

已上移 [3]: During moderate to high air temperature, a significant positive correlation was elucidated between O₃ and PM_{2.5} and the reverse negative correlation was found under low temperature.

删除的内容: The positive correlation for warm air probably reflected a formation of secondary fine particles in summer associated with high O₃. The secondary particle formation may be related to high conversion rate of SO₂ to sulfate under a high concentration of oxidants (Khoder, 2002).

已上移 [4]: Additionally, it was also associated with the formation of secondary organic aerosols with high O₃ concentrations (Kamens et al., 1999; Lambe et al., 2015; Palm et al., 2017), which was primarily produced through the photo-oxidation of BVOCs (Claeys, et al., 2004; Böge et al., 2013). As inferred above, significant emission of BVOCs was speculated around NRCS in summer.

删除的内容: The anti-correlation for cold air might be caused by the titration effect of high NO concentration, which was in relation to high primary PM_{2.5} in cold seasons. .

删除的内容: on

496 (e.g., N and NW). Trajectories belonging to S-SW and E-SE typically followed flow patterns from South Sea and Pacific
497 Ocean, respectively. Otherwise, some trajectories have short transport patterns, indicative of slow-moving air masses. Most
498 of the pollution episodes within this group are probably enriched from regional and local emission sources. Such trajectories
499 were also identified during every season in our study. For instance, the air masses associated with cluster 4 (in spring,
500 autumn, and winter) and cluster 1 in summer were predominantly originating from local areas and the nearby provinces with
501 significant pollution sources such as Jiangsu, Anhui, and Shanghai.

502 Table 3 summarizes the percentages of these identified trajectory clusters on seasonal basis and the corresponding mean
503 concentrations of PM_{2.5} and other trace gases related to each trajectory cluster. As inferred from Table 3, the clusters
504 exhibited larger variability and season dependence: the predominant clusters were W (42.66%) in spring, SW (53.89%) in
505 summer, NW (35.53%) in autumn, and N (54.91%) in winter, respectively. It's of interest to note that some trajectory
506 clusters with small percentages are remarkably related with high pollutants concentrations. In summer, a few PM_{2.5} pollution
507 cases (only 8.42% of the summertime trajectories) with mean concentration as high as 51.5 μg m⁻³ were related with the N
508 trajectories travelling across well-industrialized cities cluster (i.e., Suzhou, Wuxi, and Changzhou).

509 Furthermore, we depicted the seasonal WPSCF maps (a), the corresponding zoomed maps (b), and the emissions maps (c)
510 for PM_{2.5}, O₃, CO, NO_x, and SO₂, respectively, denoted with alphabets a, b, and c in the figure captions. Here we presented
511 the results of two representative species PM_{2.5} (Fig. 6a-6b, and 6c) and O₃ (Fig. 7a, -7b) and those of the other species
512 were included in the Supplement (Fig. S3a, -S5c). Judging from the WPSCF maps, together with their corresponding
513 zoomed views and the calculated emissions maps, a few distinct features were summarized: (1) Local emissions were both
514 significant for the primary pollutants such as CO (Fig. S3), NO_x (Fig. S4), SO₂ (Fig. S5), and PM_{2.5} (Fig. 6) on seasonal scale.
515 For O₃, local photochemistry dominated during spring, summer, and autumn (Fig. 7a, -7b) due to strong photochemical
516 reactivity; (2) The potential sources of CO and NO_x had similar patterns on spatial and seasonal scales, with higher values in
517 the NW during spring, covering the mid-YRD regions across Anhui Province and reaching the border of Henan Province; in
518 the NW and N during autumn and winter, covering the most area of Jiangsu Province and part of Shandong Province such as
519 Jinan, and Zibo city; (3) the higher values for SO₂ were located in the Ningbo city and the coast of Yellow Sea during spring,
520 in the southeastern region from East Sea during summer, probably due to ship emissions (Fan et al., 2016), but in the inland
521 cities such as Shaoxing and Quzhou city of Zhejiang Province during autumn and Anhui Province during winter. In total,
522 along with the air mass trajectories, the WPSCF maps for these primary pollutants were generally in line with their
523 respective corresponding species' emissions (Fig. 6c, -S3c, -S4c, and -S5c). Although no seasonal patterns in emission maps
524 were found, the emissions of these pollutants exhibited interspecies similarity and strong spatial dependence with
525 industrialization level.

526 In terms of PM_{2.5}, the potential sources showed distinct seasonal variations such as southeastern regions of Jiangxi
527 Province and northwestern area of Zhejiang Province during spring and in the western city of North Korea (Pyongyang) and
528 South Korea (Seoul) with the northeasterly air mass across Yellow Sea during summer. As illustrated in Fig. 6a and 6b, the
529 contributions from local emission were both found to be more significant for autumn and winter than spring and summer,

删除的内容: 9a, -9b

删除的内容: 9c

删除的内容: 10a, -10b

删除的内容: 9

删除的内容: 10a, -10b

删除的内容:) long transports from Yellow Sea, East Sea, and South Sea were also important potential sources for NO_x (Fig. S4a) and O₃ (Fig. 10a, -10b); (3

删除的内容: 4

删除的内容: 9c

删除的内容: Note that the emission of NO_x was significant from South Korea (Fig. S4c) where high WPSCF values were found in autumn (Fig. 10a), indicating a remarkable source to the surface O₃ of NRCS through the northeasterly transport.

删除的内容: 9a

删除的内容: 9b

549 covering all the cities in Zhejiang Province especially for the southern and southwestern part (e.g., Lishui, Jinhua, and
550 Quzhou city). Moreover, we found the higher WPSCF values located in the middle city of Jiangsu Province in autumn and
551 the expanded area towards the whole Jiangsu and Anhui Province and the southeast coast cities (e.g., Wenzhou, Ningbo in
552 Zhejiang Province, Fuzhou in Fujian Province) in winter, revealing the cross-boundary transport is crucial to the pollution of
553 particulate matters. This result has been confirmed by Yu et al. (2014) who also found such transport dominated in the
554 Hangzhou city during the heavy haze episode (3-9 December, 2013).

删除的内容: particle

555 For O₃, its potential sources should be interpreted with cautions since it's not directly emitted to the atmosphere and has
556 complicated chemistry involved with VOCs and NO_x. The majority of the measured O₃ is probably formed by
557 photooxidation in the vicinity of the measurement site (Fig. 7b), named as local contribution, but clear differences associated
558 with regional transport were illustrated in Fig. 7a. In spring, high O₃ concentrations were connected with air masses coming
559 from the western and southwestern region (e.g., Anhui, Jiangxi, and mid-Guangdong Province), and the northwestern area
560 such as Jiangsu, Henan, and Shandong Province; In summer, more extensive potential sources were elucidated to be located
561 in the eastern-southern-southwestern regions of China, covering the southern part of Zhejiang Province, southeastern cities
562 of Jiangxi Province, almost the whole Fujian Province, and the eastern part of Guangdong Province; the mid-Zhejiang
563 Province (e.g., Quzhou, Jinhua, and Ningbo city). A very interesting finding should be pointed out that air masses
564 transported from the offshore area of Yellow Sea, East Sea, and South Sea, respectively on southeastern Zhejiang, Jiangsu,
565 and Fujian Province, were also found to be highly relevant to the elevated O₃ at NRCS site. It was also well evidenced by
566 seasonal and spatial distributions of O₃ volume mixing ratio (VMR) simulated by MOZART-4/GEOS-5 (See the Fig. S6 in
567 the Supplement). We speculated the recirculation of pollutants by sea- and land-breeze circulations around the cities along
568 the YRD and Hangzhou Bay which has been confirmed by Li et al. (2015, 2016b), was largely responsible for the increased
569 concentration of O₃ at NRCS site. Such an increase in O₃ concentrations in urbanized coastal areas have been observed and
570 modeled in a number of studies (Oh et al., 2006; Levy et al., 2008; Martins et al., 2012). Thus, our study further emphasizes
571 the importance of local thermally induced circulation on air quality.

删除的内容: exhibited distinct seasonal and spatial distributions: apart from the local contribution as discussed above, the results with high WPSC values, as illustrated in Fig. 10a, indicated the main potential sources were located in

删除的内容: during spring

删除的内容: jinhua

删除的内容:) and the northern coastal cities (e.g., Shanghai, Lianyungang, and Dalian city) were apparently potential sources in autumn; in regard to winter, long distant transport acted as a significant source of surface O₃, specifically from the northeasterly air mass Yellow Sea.

删除的内容: China

删除的内容: Yellow China Sea, or even far from

删除的内容: China

删除的内容: significant sources of

删除的内容: throughout

删除的内容: year.

572 3.5 Cases studies for haze (high PM_{2.5}) and photochemical pollution (high O₃) episodes

573 To elucidate the specific causes of high PM_{2.5} and O₃ episodes including the transport and local photochemical formation, we
574 chose two typical cases for detailed interpretations and are presented here. In this study, the haze pollution episode is defined
575 as the event that continuous days with daily averaged PM_{2.5} concentration exceeding 75 μg m⁻³, which has been also used to
576 distinguish non-haze and haze episode in other studies (Yu et al., 2014; Wu et al., 2016a). With respect to this campaign,
577 there were two non-haze episodes (Phase I (28 Nov.-3 Dec.), II (10-12 Dec.)), and their subsequent severe haze pollution
578 episodes (Phase III (2-9 Dec.) and IV (13-15 Dec.)) at NRCS site, respectively, as illustrated in Fig. 8. In the Phase III, it
579 showed that high PM_{2.5} (up to 406 μg m⁻³) appeared on 7 December and board PM_{2.5} peaks (around 300 μg m⁻³) occurred
580 before and after two days. Simultaneously, CO, SO₂, and NO_x also reached very high levels on this day, confirming that the
581 common origin of CO and PM_{2.5} from heating and combustion and the rapid conversion of SO₂ and NO_x to sulfate and

删除的内容: 11

606 nitrate in PM_{2.5} in winter. But for O₃, its level reached as low as 11.5 ppbv at 15:00 LT on that day, owing to the weak
607 photochemical activity under the severe haze pollution. Along with the high NO₂ concentration (around 120 ppbv), it could
608 not produce sufficient conversion oxidants (OH and HO₂ radicals) for the gas-phase oxidation of SO₂ (Poppe et al., 1993;
609 Hua et al., 2008), while the increased relative humidity during 6-8 December possibly favored the aqueous phase oxidation
610 of SO₂.

611 Moreover, according to the results obtained from the backward trajectory cluster and WSPCF analysis during 2-9
612 December, 2013 (Fig. S7 in the Supplement), we found an apparent contribution from the transported air mass from
613 northwest region such as Jiangsu Province and Anhui Province. Our results were in good agreement with contemporaneous
614 measurement in Hangzhou (Wu et al., 2016a). Subsequently, at the end of this episode significant drops of these species
615 except O₃ were observed from 00:00 LT to 23:00 LT on 9 December (i.e., 189 to 41.6 µg m⁻³ for PM_{2.5}, 2.3 to 1.0 ppmv for
616 CO, and 145 to 47.9 ppbv for NO_x). Weather chart and wind data suggested that the region of NRCS was always controlled
617 by a strong continental high pressure system originating from northwest before 8 December (Fig. 9a-9f), but rapidly changed
618 to be dominated under a strong marine high pressure system coming from east at 02:00 LT on 9 December (Fig. 9g-9h),
619 which brought clean maritime air passing over Yellow Sea and thus caused such decreases in these pollutants. However, it
620 quickly turned back to be controlled under a continental high pressure system described above, carrying pollutants from the
621 city clusters to the NRCS site. It could account for the accumulations of these species during the intermediate period (Phase
622 II). For the subsequent Phase IV with high PM_{2.5} episode it was also found to be governed by a stagnant high pressure over
623 YRD region (Fig. S8).

624 For the photochemical pollution events, we selected three cases with O₃ exceedances (74.6 ppbv) during May-August
625 according to Grade II standard of CAAQS. As displayed in Fig. 10, they were the Phase I (28-30 May and 20-22 June) with
626 rapid buildup and decrease of O₃ within 3 days, Phase II (9-12 July) representing a distinct accumulation process of O₃
627 exceedances, and the Phase III (1-3 May, 20-22 May, and 9-11 August) with high O₃ levels within three consecutive days.
628 For 28 May in the Phase I, weather chart suggested that a strong anticlockwise cyclone located over YRD. In this case, the
629 cyclone (i.e., low pressure) caused favoring conditions, e.g., cloudy weather and high wind velocities, for pollution diffusion.
630 Then, a strong clockwise anticyclone from northwest, sweeping over cities cluster (i.e., Nanjing and Shanghai), rapidly
631 moved adjacent to NRCS site on 29 May. It carried the primary pollutants such as CO, SO₂, NO_x from these megacities and
632 secondary products (i.e., O₃ and some NO₂) were further produced via complex photochemical reactions under such synoptic
633 conditions. As orange shaded area shown in Fig. 10, the hourly maximums of O₃ and PM_{2.5} were observed as high as 141.2
634 ppbv and 135.8 µg m⁻³ at 13:00 LT on 29 May. Following this day, the cyclone again dominated this region and caused
635 sudden decreased in atmospheric pollutants. Also, similar case was found during 20-22 June under such changes in synoptic
636 weather. For Phase II (9-12 July), a typical accumulation process was observed with the daily maximums of atmospheric
637 pollutants increasing from 90.4 to 142.9 ppbv for O₃, 77.6 to 95.3 µg m⁻³ for PM_{2.5}, and 80.2 to 125.2 ppbv for NO_y,
638 respectively. The examination of day-to-day 925-hPa synoptic chart derived from NECP reanalysis suggested that high
639 pressure system governed over YRD during 9-11 July, with southwesterly prevailing wind. The air masses recorded at this

删除的内容: S6

删除的内容: 12a-12f

删除的内容: 12g-12h

删除的内容: S7

删除的内容: as depicted in Section 3.1.

删除的内容: 13

删除的内容: 13

647 site mainly came from the most polluted city clusters in the southwest (e.g. Zhejiang, Jiangxi, and Fujian Province).
648 Meanwhile, the stagnant synoptic condition (i.e., low wind speed) favored the accumulation of primary pollutants such as
649 CO and NO_x. For secondary pollutants O₃ and PM_{2.5}, they were also rapidly formed via photochemical oxidation and further
650 accumulated under such synoptic condition, together with continuous high-temperature (daily mean around 33 °C). On 12
651 July, a typhoon (No. 7 Typhoon Soulik) moved to a location a few hundred kilometers away from NRCS site, bringing
652 southeasterly maritime air over YRD. Daily maximum O₃ reached at 142.8 ppbv at 12:00 LT even with low concentration of
653 precursors (i.e., 0.48 ppmv for CO and 16.0 ppbv for NO_x), suggesting high photochemical production efficiency of O₃ in
654 this region in summer. This phenomenon has been also found in the multi-day episode of high O₃ in Nanjing during 20-21
655 July, 2011 (Ding et al., 2013). In this phase, PM_{2.5} mass concentration showed very good correlation (R = 0.79, p < 0.001)
656 with O₃ during the daytime (09:00-17:00 LT), possibly indicating a common origin of BVOCs due to the significant
657 vegetation emission as discussed above, in addition to high biomass production in the southern part of the YRD (Ding et al.,
658 2013). For Phase III (1-3 May, 20-22 May, and 9-11 August), there were most sunny days with low wind speed and
659 moderate/high air temperature which were both beneficial factors for photochemical formation of O₃, together with sufficient
660 precursors (NO_x and VOCs) in the summer and early autumn over YRD. For 1-3 May and 20-22 May, daily maximum T
661 were moderate (around 25 °C versus 31 °C), while the daily maximums NO_x reached as high as 43-95 ppbv and 50-90 ppbv,
662 respectively, which both favoring the photochemical formation to produce the continuous high O₃ concentrations (daily
663 maximums: 96-133 ppbv via 104-133 ppbv). The reverse case is also true during 9-11 August, on which the daily maximum
664 T and NO_x ranged from 40.6-41.4 °C and 33-44 ppbv, respectively, resulting in producing continuously high O₃ from 98.8
665 ppbv to 130.5 ppbv.

666 **3.6 Photochemical age and ozone production efficiency during photochemical pollution and haze period**

667 Photochemical age is often used to express the extent of photochemistry, which can be estimated using some indicator such
668 as NO_x/NO_y (Carpenter et al., 2000; Lin et al., 2008, 2009, 2011; Parrish et al., 1992). Air masses with fresh emissions have
669 NO_x/NO_y close to 1, while lower NO_x/NO_y ratio for the photochemical aged air masses. In this study, for the haze events as
670 mentioned above, the average and maximum NO_x/NO_y ratios were as high as 0.80 and 0.99, respectively, indicating that
671 photochemical conversion of NO_x is not absent but fairly slow. It was well consistent with the largely weaken
672 photochemistry due to the low intensity of UV radiation in winter. In contrast, during the photochemical pollution period,
673 they were low as 0.53 and 0.14 for the average and minimum ratio. The simultaneous measurements of atmospheric O₃, NO_x,
674 and NO_y can provide an insight into calculating the ozone production efficiency (OPE) for different seasons. From the data
675 of O_x and NO_z, the ratio of Δ(O_x)/Δ(NO_z) can be calculated as a kind of observation-based OPE (Trainer et al., 1993; Sillman,
676 2000; Kleinman et al., 2002; Lin et al., 2011;). In this study, the mean values of NO_z and O_x between 07:00-15:00 LT, were
677 used to calculate the OPE values through the linear regressions. In addition, these data were also confined to the sunny days
678 and the wind speed below 3 m s⁻¹, reflecting the local photochemistry as possible. The OPE value during the photochemical
679 pollution period (SOPE) as mentioned above was 1.99, generally within the reported range of 1-5 in the PRD cities, but

680 lower than 3.9-9.7 in summer Beijing (Chou et al., 2009; Ge et al., 2012). Meanwhile, the OPE value of 0.77 during the haze
681 period (HPOE) was also comparable with the reported value of 1.1 in winter in Beijing (Lin et al., 2011). The smaller winter
682 OPE value in Hangzhou might be ascribed to the weaker photochemistry and higher NO_x concentration. At high NO_x level,
683 OPE tends to decrease with the increased NO_x concentration (Ge et al., 2010; Lin et al., 2011). In Hangzhou, the NO_x level is
684 frequently higher than needed for producing photochemical O₃, and excessive NO_x causes net O₃ loss rather than
685 accumulation. In this study, 75% of daily OPE values were negative, for which two factors could be accounted. To some extent,
686 due to the geographical location and unique climate characteristic for Hangzhou as depicted above, the interference of
687 unbeneficial meteorological condition existed in the formation of local O₃ deriving from photochemistry, i.e., strong wind,
688 frequent rainy days. The other one is because of the consumption of O₃ by excessive NO_x, which was also well confirmed by
689 the conclusion that Hangzhou was mostly in the VOCs-limited regime as discussed in Section 3.2. Such circumstance was
690 also observed at the rural site Gucheng in the NCP and in Beijing urban area (Lin et al., 2009, 2011). Taking the average of
691 SOPE of 1.99 and the average daytime increment of NO_z (ca. 20 ppbv), we estimated an average photochemical O₃
692 production of about 39.8 ppbv during photochemical pollution period. In contrast, the lower average photochemical O₃
693 production was estimated to be 10.78 ppbv during haze period based on HOPE, which might act as a significant source for
694 surface O₃ in winter in Hangzhou.

695 4 Conclusions

696 In this study, we presented an overview of one year measurements of trace gases (O₃, CO, NO_x, NO_y, and SO₂) and
697 particulate matters (PM_{2.5} and PM₁₀) at National Reference Climatological Station in Hangzhou. The characteristics and
698 cause of these chemicals were investigated by their seasonal characteristics, along the comparison with the previous results
699 in other regions in China, interspecies correlations, and the concentration dependence on local emission and regional
700 transport. Specific photochemical pollution and haze case were studied in detail based on discussing the physical process and
701 photochemical formation (ozone production efficiency). The main findings and conclusions are summarized below:

702 a) Within one year study period, there were 38 days of O₃ exceedances and 62 days of PM_{2.5} exceedances of the National
703 Ambient Air Quality Standards in China at the site, suggesting heavy air pollution in this region. In general, the
704 concentration levels of these chemicals were consistent with those observed by other contemporaneous measurements in
705 Hangzhou and the other cities in YRD, but lower than those in NCP. Distinct seasonal characteristics were found with a
706 board peak in late spring and middle summer and a minimum in winter for O₃, while with maximum in winter and minimum
707 in summer for PM_{2.5}.

708 b) A positive O₃-NO_y correlation was found for air masses with high air temperature in summer, suggesting a strong local
709 photochemical production of O₃. In addition, correlation analysis shows an important conversion of SO₂ to sulfate and NO_x
710 to nitrate and/or deposition in the humid condition. CO-NO_y-O₃ correlation suggested a VOC-limited regime for the overall
711 study period but moved toward an optimum O₃ production zone during warm seasons. The positive correlation between O₃
712 and PM_{2.5} under high air temperature indicated a formation of secondary fine particulates in warm seasons, respectively.

删除的内容: particle

删除的内容: particles

715 c) The results from the emission inventories of the primary pollutants such as PM_{2.5}, CO, NO_x, and SO₂ demonstrated that
716 local emissions were both significant for these species but without distinct seasonal variations. The major potential sources
717 of PM_{2.5} were located in the regions of southwesterly in spring, northwesterly and northeasterly in summer, and
718 northwesterly (the whole Jiangsu Province and Anhui Province) in autumn and winter, respectively. For CO and NO_x, they
719 showed similar patterns with northwestern regions covering the mid-YRD regions and Anhui Province during spring and in
720 the northwestern and northern regions including Jiangsu Province and part of Shandong Province during autumn and winter.
721 The distinct seasonal variation in SO₂ potential might be from southwestern and eastern region during spring and summer
722 but northwestern during autumn and winter. Air masses transported from the offshore area of Yellow Sea, East Sea, and
723 South Sea, respectively on southeastern Zhejiang, Jiangsu, and Fujian Province, were also found to be highly relevant to the
724 elevated O₃ at NRCS site, probably due to the recirculation of pollutants by sea- and land-breeze circulations around the
725 cities along the YRD and Hangzhou Bay. This finding further emphasizes the importance of urban-induced circulation on air
726 quality.

删除的内容: important in increasing surface

727 d) Case studies for photochemical pollution and haze episodes both suggest the combined importance of local atmospheric
728 photochemistry and synoptic weather during the accumulation (related with anticyclones) and dilution process (related with
729 cyclones) of these episodes. The average photochemical O₃ productions were estimated to be 39.8 and 10.78 ppbv during
730 photochemical pollution and haze period, respectively, indicating local photochemistry might act as a significant source for
731 surface O₃ in winter in Hangzhou.

732 Our study further completes a picture of air pollution in the YRD, interprets the physical and photochemical processes
733 during haze and photochemical pollution episodes, and explores the seasonal and spatial variations in the potential sources of
734 these pollutants. Moreover, this work suggests the cross-region control measures are crucial to improve air quality in the
735 YRD region, and further emphasizes the importance of local thermally induced circulation on air quality.

736 **Acknowledgement.** This study is financially supported by National Key Research and Development Program of China
737 (2016YFC0202300), National Natural Science Foundation of China (41775127, 41505108, and), and Shanghai Key
738 Laboratory of Meteorology and Health (QXJK201501). The authors are especially grateful to Dr. Miao Yucong for the
739 technical supports in drawing a part of figures and discussions.
740

带格式的: 字体: 加粗, 倾斜

带格式的: 定义网格后不调整右缩进, 不对齐到网格

删除的内容: Natural Science Foundation of China (41505108 and 41775127), National

741 References

742 Atkinson, R.: Atmospheric chemistry of VOCs and NO_x. Atmos. Environ., 34, 2063-2101, 2000.
743 Böge, O., Mutzel, A., Linuma, Y., Yli-Pirilä, P., Kahnt, A., Joutsensaari, J., and Herrmann, H.: Gas-phase products and
744 secondary organic aerosol formation from the ozonolysis and photooxidation of myrcene, Atmos. Environ., 79, 553-560,
745 2013.

已移动(插入) [5]

带格式的: 字体: AdvOT863180fb, 字体颜色: 黑色

751 Calfapietra, C., Fares, S., Manes, F., Morani, A., Sgrign, G., and Loreto, F.: Role of biogenic volatile organic compounds
752 (BVOC) emitted by urban trees on ozone concentration in cities: A review, *Environ. Poll.*, 183, 71-80, 2013.

753 Cao, J., Shen, Z., Chow, J. C., Qi, G., and Watson, J. G.: Seasonal variations and sources of mass and chemical composition
754 for PM₁₀ aerosol in Hangzhou, China, *Particuology*, 7, 161-168, 2009.

755 Carpenter, L. J., Green, T. J., Mills, G. P., Bauguitte, S., Penkett, S. A., Zanis, P., Schuepbach, E., Schmidbauer, N., Monks,
756 P. S., and Zellweger, C.: Oxidized nitrogen and ozone production efficiencies in the springtime free troposphere over
757 the Alps, *J. Geophys. Res.*, 105, 14547-14559, 2000.

758 Chai, F. H., Gao, J., Chen, Z. X., Wang, S. L., Zhang, Y. C., Zhang, J. Q., Zhang, H. F., Yun, Y. R., and Ren, C.: Spatial and
759 temporal variation of particulate matter and gaseous pollutants in 26 cities in China, *J. Environ. Sci.*, 26, 75-82, 2014.

760 Chang, J., Ren, Y., Shi, Y., Zhu, Y. M., Ge, Y., Hong, S. M., Jiao, L., Lin, F. M., Peng, C. H., Mochizuki, T., Tani, A., Mu,
761 Y., and Fu, C. X.: An inventory of biogenic volatile organic compounds for a subtropical urban-rural complex, *Atmos.*
762 *Environ.*, 56, 115-123, 2012.

763 Chen, T., He, J., Lu, X., She, J., and Guan, Z.: Spatial and temporal variations of PM_{2.5} and its relation to meteorological
764 factors in the urban area of Nanjing, China, *Int. J. Environ. Res. Pub. Heal.*, 13, 921, 2016.

765 Cheng, Y. F., Zheng, G. J., Wei, C., Mu, Q., Zheng, B., Wang, Z. B., Gao, M., Zhang, Q., He, K. B., Carmichael, G., Pöschl,
766 U., and Su, H.: Reactive nitrogen chemistry in aerosol water as a source of sulfate during haze events in China, *Sci.*
767 *Adv.*, 2, 12, 1-11, 2016.

768 Chou, C. K., Tsai, C. Y., Shiu, C. J., Liu, S. C., and Zhu, T.: Measurement of NO_y during campaign of air quality research in
769 Beijing 2006 (CAREBeijing-2006): implications for the ozone production efficiency of NO_x, *J. Geophys. Res.*, 114, 1,
770 328-334, 2009.

771 | Chow, J. C. and Watson, J. G.: Review of PM_{2.5} and PM₁₀ apportionment for fossil fuel combustion and other sources by the
772 chemical mass balance receptor model, *Energy Fuels*, 16, 2, 222-260, 2002.

773 Claeys, M., Graham, B., Vas, G., Wang, W., Vermeylen, R., Pashynska, V., Cafmeyer, J., Guyon, P., Andreae, M. O.,
774 Artaxo, P., and Maenhaut, W.: Formation of secondary organic aerosols through photooxidation of isoprene, *Science*,
775 303, 5661, 1173-1176, 2004.

776 Dickerson, R. R., Kondragunta, S., Stenchikov, G., Civerolo, K. L., Doddridge, B. G., and Holben, B. N.: The Impact of
777 aerosols on solar ultraviolet radiation and photochemical pollution, *Science*, 278, 5339, 827-830, 1997.

778 | Ding, A. J., Wang, T., Thouret, V., Cammas, J.-P., and Nédélec, P.: Tropospheric ozone climatology over Beijing: analysis
779 of aircraft data from the MOZAIC program, *Atmos. Chem. Phys.*, 8, 1-13, 2008.

780 Ding, A. J., Fu, C. B., Yang, X. Q., Sun, J. N., Zheng, L. F., Xie, Y. N., Herrmann, E., Nie, W., Petäjä, T., Kerminen, V. M.,
781 | and Kulmala, M.: Ozone and fine particulate in the western Yangtze River Delta: an overview of 1 yr data at the
782 SORPES station, *Atmos. Chem. Phys.*, 13, 5813-5830, 2013.

带格式的: 下标

带格式的: 下标

删除的内容: 'ed'elec

删除的内容: particule

785 Fan, Q., Zhang, Y., Ma, W., Ma, H., Feng, J., Yu, Q., Yang, X., Ng, S.K.W., Fu, Q., and Chen, L.: Spatial and seasonal
786 dynamics of ship emissions over the Yangtze River Delta and East China Sea and their potential environmental
787 influence, *Environ. Sci. Technol.*, 50, 1322-1329, 2016.

788 Feng, Z. Z., Sun, J. S., Wan, W. X., Hu, E. Z., and Calatayud, V.: Evidence of widespread ozone-induced visible injury on
789 plants in Beijing, China, *Environ. Pollut.*, 193, 296-301, 2014.

790 Ge, B. Z., Xu, X. B., Lin, W. L., and Wang, Y.: Observational study of ozone production efficiency at the Shangdianzi
791 regional background station, *Environ. Sci.*, 31, 7, 1444-1450, 2010 (In Chinese with English abstract).

792 Ge, B. Z., Xu, X. B., Lin, W. L., Li, J., and Wang, Z. F.: Impact of the regional transport of urban Beijing pollutants on
793 downwind areas in summer: ozone production efficiency analysis, *Tellus*, 64, 17348, 2012.

794 Geng, F. H., Zhao, C. S., Tang, X., Lu, G. L., and Tie, X. X.: Analysis of ozone and VOCs measured in Shanghai: A case study,
795 *Atmos. Environ.*, 41, 989-1001, 2007.

796 Guenther, A., Hewitt, C. N., Erickson, D., Fall, R., Geron, C., Graedel, T., Harley, P., Klinger, L., Lerdau, M., McKay, W.
797 A., Pierce, T., Scholes, B., Steinbrecher, R., Tallamraju, R., Taylor, J., and Zimmerman, P. L.: A global model of
798 natural volatile organic compound emissions, *J. Geophys. Res.*, 100, 8873-8892, 1995.

799 Guo, H., Wang, T., Simpson, I., J., Blake, D. R., Yu, X., M., Kwok, Y. H., and Li, Y. S.: Source contributions to ambient
800 VOCs and CO at a rural site in eastern China, 38(27), 4551-4560, 2004.

801 He, K. B., Huo, H., and Zhang, Q.: Urban air pollution in China: current status, characteristics, and progress, *Annu. Rev.*
802 *Energ. Env.*, 27, 397-431, 2002.

803 Hsu, Y.K., Holsen, T. M., and Hopke, P. K.: Comparison of hybrid receptor models to locate PCB sources in Chicago,
804 *Atmos. Environ.*, 37, 545-562, 2003.

805 Hua, W., Chen, Z. M., Jie, C. Y., Kondo, Y., Hofzumahaus, A., Takegawa, N., Chang, C. C., Lu, K. D., Miyazaki, Y., Kita,
806 K., Wang, H. L., Zhang, Y. H., and Hu, M.: Atmospheric hydrogen peroxide and organic hydroperoxides during
807 PRIDE-PRD'06, China: their concentration, formation mechanism and contribution to secondary aerosols, *Atmos.*
808 *Chem. Phys.*, 8, 6755-6773, 2008.

809 Huang, Y., Shen, H. Z., Chen, H., Wang, R., Zhang, Y. Y., Su, S., Chen, Y. C., Lin, N., Zhao, S. J., Zhong, Q. R., Wang, X.
810 L., Liu, J. F., Li, B. G., Liu, W. X., and Tao, S.: Quantification of global primary emissions of PM_{2.5}, PM₁₀, and TSP
811 from combustion and industrial process sources, *Environ. Sci. Technol.*, 48, 13834-13843, 2014.

812 IPCC, Summary for Policymakers. In *Climate Change 2007: The Physical Science Basis*. Contribution of Working Group I
813 to the Fourth Assessment Report of the Intergovernmental Panel on Climate Change; Solomon, S., Qin, D., Manning,
814 M., Chen, Z., Marquis, M., Averyt, K. B., Tignor, M., Miller, H. L., Eds.; Cambridge University Press: Cambridge,
815 United Kingdom and New York, NY, USA, 2007.

816 Jansen, R. C., Shi, Y., Chen, J. M., Hu, Y. J., Xu, C., Hong, S. M., Jiao, L., and Zhang, M.: Using hourly measurements to
817 explore the role of secondary inorganic aerosol in PM_{2.5} during haze and fog in Hangzhou, China, Adv. Atmos. Sci., 31,
818 1427-1434, 2014.

已移动(插入) [6]

已移动(插入) [7]

带格式的: 字体颜色: 自动设置

已移动(插入) [8]

带格式的: 字体颜色: 自动设置

已移动(插入) [9]

已移动(插入) [10]

删除的内容: Jaffe, D. A., Mahura, A.,
Kelley,

821 [Kamens, R., Jang, M., Chien, C.J., and Leach, K.: Aerosol formation from reaction of \$\alpha\$ -pinene and ozone using a gas-phase](#)
822 [kinetics-aerosol partitioning model, Environ. Sci. Technol., 33, 1430-1438, 1999.](#)

823 [Kang, H., Zhu, B., Su, J., Wang, H., Zhang, Q., and Wang, F.: Analysis of a long-lasting haze episode in Nanjing, China,](#)
824 [Atmos. Res., 120-121, 78-87, 2013.](#)

825 [Khoder, M. I.: Atmospheric conversion of sulfur dioxide to particulate sulfate and nitrogen dioxide to particulate nitrate and](#)
826 [gaseous nitric acid in an urban area, Chemosphere, 49, 675-684, 2002.](#)

827 [Kleinman, L., Daum, P. H., Lee, Y.-N., Nunnermacker, L. J., Springston, S. R., Weinstein-Lloyd, J., and Rudolph, J.: Ozone](#)
828 [production efficiency in an urban area, J. Geophys. Res., 107, 4733, 2002.](#)

829 [Lambe, A. T., Chhabra, P. S., Onasch, T. B., Brune, W. H., Hunter, J. F., Kroll, J. H., Cummings, M. J., Brogan, J. F.,](#)
830 [Parmar, Y., Worsnop, D. R., Kolb, C. E., and Davidovits, P.: Effect of oxidant concentration, exposure time, and seed](#)
831 [particulates on secondary organic aerosol chemical composition and yield, Atmos. Chem. Phys., 15, 3063-3075, 2015.](#)

832 [Levy, I., Dayan, U., and Mahrer, Y.: A five-year study of coastal recirculation and its effect on air pollutants over the east](#)
833 [Mediterranean region, J. Geophys. Res., 113, D16121, 2008.](#)

834 [Li, M. M., Mao, Z. C., Song, Y., Liu, M. X., and Huang, X.: Impact of the decadal urbanization on thermally induced](#)
835 [circulations in eastern China, J. Appl. Meteorol. Clim., 54, 259-282, 2015.](#)

836 [Li, L., An, J. Y., Shi, Y. Y., Zhou, M., Yan, R. S., Huang, C., Wang, H. L., Lou, S. R., Wang, Q., Lu, Q., and Wu, J.: Source](#)
837 [apportionment of surface ozone in the Yangtze River Delta, China in the summer of 2013, Atmos. Environ., 144, 194-](#)
838 [207, 2016a.](#)

839 [Li, M. M., Song, Y., Mao, Z. C., Liu, M. X., and Huang, X.: Impact of thermal circulations induced by urbanization on](#)
840 [ozone formation in the Pearl River Delta, China, Atmos. Environ., 127, 382-392, 2016b.](#)

841 [Li, K. W., Chen, L. H., Ying, F., White, S. J., Jang, C., Wu, X. C., Gao, X., Hong, S. M., Shen, J. D., Azzi, M., and Cen, K.](#)
842 [F.: Meteorological and chemical impacts on ozone formation : A case study in Hangzhou, China, Atmos. Res., doi:](#)
843 [10.1016/j.atmosres.2017.06.003, 2017.](#)

844 [Lin, W. L., Xu, X. B., Zhang, X. C., and Tang, J.: Contributions of pollutants from North China Plain to surface ozone at the](#)
845 [Shangdianzi GAW Station, Atmos. Chem. Phys., 8, 5889-5898, 2008.](#)

846 [Lin, W. L., Xu, X. B., Ge, B. Z., and Zhang, X. C.: Characteristics of gaseous pollutants at Gucheng, a rural site southwest](#)
847 [of Beijing, J. Geophys. Res., 114, 4723-4734, 2009.](#)

848 [Lin, W. L., Xu, X. B., Ge, B. Z., and Liu, X.: Gaseous pollutants in Beijing urban area during the heating period 2007-2008:](#)
849 [variability, sources, meteorological, and chemical impacts, Atmos. Chem. Phys., 11, 8157-8170, 2011.](#)

850 [Liu, G., Li, J., H., Wu, D., and Xu, H.: Chemical composition and source apportionment of the ambient PM_{2.5} in Hangzhou,](#)
851 [China, Particuology, 18, 135-143, 2015.](#)

852 [Liu, T., Li, T. T., Zhang, Y. H., Xu, Y. J., Lao, X. Q., Rutherford, S., Chu, C., and Luo, Y.: The short-term effect of ambient](#)
853 [ozone on mortality is modified by temperature in Guangzhou, China, Atmos. Environ., 76, 59-67, 2013.](#)

已上移 [6]: J.,

已上移 [8]: C.,

带格式的: 字体颜色: 自动设置

删除的内容: Atkins, J., Novelli, P.

带格式的: 字体颜色: 自动设置

删除的内容: and Merrill, J.: Impact of Asian emissions on the remote North Pacific atmosphere: interpretation of CO data from Shemya, Guam, Midway, and Mauna Loa, J. Geophys. Res., 101, 2037-2048, 1997. .

删除的内容: _-

删除的内容: Kato, N. and Akimoto, H.: Anthropogenic emissions of SO₂ and NO_x in Asia: emission inventories, Atmos. Environ., 26, 19, 2997-3017, 1994. .

删除的内容: -

删除的内容: particles

已移动(插入) [11]

870 Logan, J. A.: Tropospheric ozone: Seasonal behavior, trends, and anthropogenic influence. *J. Geophys. Res.*, 90, 10463-
871 10482, 1985.

872 Luo, C., St. John, J. C., Zhou, X. J., Lam, K. S., Wang, T., and Chameides, W. L.: A nonurban ozone air pollution episode
873 over eastern China: observations and model simulations, *J. Geophys. Res.*, 105, 1889-1908, 2000.

874 Ma, Z. W., Hu, X. F., Sayer, A. M., Levy, R., Zhang, Q., Xue, Y. G., Tong, S. L., Bi, J., Huang, L., and Liu, Y.: Satellite-
875 based spatiotemporal trends in PM_{2.5} concentrations: China, 2004-2013, *Environ. Health Persp.*, 124, 184-192, 2016.

876 Martins, D. K., Stauffer, R. M., Thompson, A. M., Knepp, T. N., and Pippin, M.: Surface ozone at a coastal suburban site in
877 2009 and 2010: relationships to chemical and meteorological processes, *J. Geophys. Res.*, 117, D5, 5306, 2012.

878 Meagher, J. F., Stockburger, L., Bailey, E. M., and Huff, O.: The oxidation of sulfur dioxide to sulfate aerosols in the plume
879 of a coal-fired power plant, *Atmos. Environ.*, 12, 11, 2197-2203, 1978.

880 Mercado, L. M. Bellouin, N. Sitch, S. Boucher, O. Huntingford, C. Wild, M. and Cox, P. M.: Impact of changes in diffuse
881 radiation on the global land carbon sink, *Nature*, 458, 7241, 1014-1017, 2009.

882 Miao, Y. C., Liu, S. H., Zheng, Y. J., Wang, S., Liu, Z. X., and Zhang, B. H.: Numerical study of the effects of planetary
883 boundary layer structure on the pollutant dispersion within built-up areas, *J. Environ. Sci.*, 32, 168-179, 2015a.

884 Miao, Y. C., Hu, X. M., Liu, S. H., Qian, T., Xue, M., Zheng, Y., and Wang, S.: Seasonal variation of local atmospheric
885 circulations and boundary layer structure in the Beijing-Tianjin-Hebei region and implications for air quality, *J. Adv.
886 Model. Earth Syst.*, 7, 1, 1-25, 2015b.

887 Miao, Y. C., Guo, J. P., Liu, S. H., Liu, H., Zhang, G., Yan, Y., and He, J.: Relay transport of aerosols to Beijing-Tian-Hebei
888 region by multi-scale atmospheric circulations, *Atmos. Environ.*, 165, 35-45, 2017a.

889 Miao, Y. C., Guo, J. P., Liu, S. H., Liu, H., Li, Z. Q., Zhang, W. C., and Zhai, P. M.: Classification of summertime synoptic
890 patterns in Beijing and their associations with boundary structure affecting aerosol pollution, *Atmos. Chem. Phys.*, 17,
891 3097-3110, 2017b.

892 Ministry of Environmental Protection of China (MEP), Ambient air quality standards (GB 3095-2012), 12 pp., China
893 Environmental Science Press, Beijing, 2012 (in Chinese).

894 Oh, I. B., Kim, Y. K., Lee, H. W., and Kim, C. H.: An observational and numerical study of the effects of the late sea breeze
895 on ozone distributions in the Busan metropolitan area, Korea, *Atmos. Environ.*, 40, 1284-1298, 2006.

896 Palm, B. B., Campuzano-Jost, P., Day, D. A., Ortega, A. M., Fry, J. L., Brown, S. S., Zarzana, K. J., Dube, W., Wagner, N.
897 L., Draper, D. C., Kaser, L., Jud, W., Karl, T., Hansel, A., Gutiérrez-Montes, C., and Jimenez, J. L.: Secondary organic
898 aerosol formation from in situ OH, O₃, and NO₃ oxidation of ambient forest air in an oxidation flow reactor, *Atmos.
899 Chem. Phys.*, 17, 5331-5354, 2017.

900 Parrish, D. D., Hahn, C. J., Williams, E. J., Borton, R. B., Fehsenfeld, F. C., Singh, H. B., Shetter, J. D., Gandrud, B. W., and
901 Ridley, B. A.: Indications of photochemical histories of Pacific air masses from measurements of atmospheric trace
902 species at Point Arena, California, *J. Geophys. Res.*, 97, 15883-15901, 1992.

删除的内容: Xiuji, Z

904 | Polissar, A.V., Hopke, P.K., Paatero, P., Kaufmann, Y.J., Hall, D.K., Bodhaine, B.A., Dutton, E.G. and Harris, J.M.: The
905 | aerosol at Barrow, Alaska: long-term trends and source locations. Atmos. Environ., 33, 2441-2458, 1999.

906 | Pope, C. and Dockery, D.: Epidemiology of particulate effects. In Air pollution and health; Holgate, S. T., Koren, H. S.,
907 | Samet, J. M., Maynard, R. L., Eds.; Academic Press: San Diego; 673-705, 1999.

908 | Poppe, D., Wallasch, M., and Zimmermann, J.: The dependence of the concentration of OH on its precursors under
909 | moderately polluted conditions: a model study, J. Atmos. Chem., 16, 61-78, 1993.

910 | Qi, B., Du, R., Yu, Z., Zhou, B., and Yuan, X.: Characteristics of atmospheric fine particulates concentrations in Hangzhou
911 | region, Environ. Chem., 34, 77-82, 2015.

912 | Qi, H. X., Lin, W. L., Xu, X. B., Yu, X. M., and Ma, Q. L.: Significant downward trend of SO₂ observed from 2005 to 2010
913 | at a background station in the Yangtze Delta region, China, Sci. China Chem., 55, 7, 1451-1458, 2012.

914 | Ravishankara, A. R.: Heterogeneous and multiphase chemistry in the troposphere, Science, 276, 1058-1065, 1997.

915 | Roelofs, G. J. and Lelieveld, J.: Model study of the influence of cross-tropopause O₃ transports on tropospheric O₃ levels,
916 | Tellus B, 49, 38-55, 1997.

917 | Saxena, P. and Seigneur, C.: On the oxidation of SO₂ to sulfate in atmospheric aerosols, Atmos. Environ., 21, 4, 807-812,
918 | 1987.

919 | Seinfeld, J. H., Carmichael, G. R., Arimoto, R., Conant, W. C., Brechtel, F. J., Bates, T. S., Cahill, T. A., Clarke, A. D.,
920 | Doherty, S. J., Flatau, P. J., Huebert, B. J., Kim, J., Markowicz, K. M., Quinn, P. K., Russell, L. M., Russell, P. B.,
921 | Shimizu, A., Shinozuka, Y., Song, C. H., Tang, Y. H., Uno, I., Vogelmann, A. M., Weber, R. J., Woo, J. H., and Zhang,
922 | X. Y.: ACE-ASIA - Regional climatic and atmospheric chemical effects of Asian dust and pollution. Bull. Am.
923 | Meteorol. Soc., 85, 3, 367-380, 2004.

924 | Seinfeld, J. H. and Pandis, S. N.: Atmospheric Chemistry and Physics: From Air Pollution to Climate Change, 2nd ed., John
925 | Wiley & Sons: New York, USA, 57-58 and 381-383, 2006

926 | Seltenrich, N.: A clearer picture of China's air using satellite data and ground monitoring to estimate PM_{2.5} over time,
927 | Environ. Health Persp., 124, A38, 2016.

928 | Shao, M., Tang, X. Y., Zhang, Y. H., and Li, W. J.: City clusters in China: air and surface water pollution, Front. Ecol.
929 | Environ., 4, 7, 353-361, 2006.

930 | Sillman, S.: Ozone production efficiency and loss of NO_x in power plant plumes: photochemical model and interpretation of
931 | measurements in Tennessee, J. Geophys. Res., 105, 9189-9202, 2000.

932 | Streets, D. G., Fu, J. S., Jang, C. J., Hao, J. M., He, K. B., Tang, X. Y., Zhang, Y. H., Wang, Z. F., and Li, Z. P.: Air quality
933 | during the 2008 Beijing Olympic Games, Atmos. Environ., 41, 480-492, 2007.

934 | Su, S., Li, B. G., Cui, S. Y., and Tao, S.: Sulfur dioxide emissions from combustion in China: from 1990 to 2007, Environ.
935 | Sci. Technol., 45, 8403-8410, 2011.

删除的内容: Parrish, D. D., Trainer,

已上移 [7]: M.,

删除的内容: Holloway, J. S., Yee, J. E., Warshawsky, M. S., and Fehsenfeld, F. C.: Relationships between ozone and carbon monoxide at surface sites in the North Atlantic region, J. Geophys. Res., 103, 13357-13376, 1998. .

删除的内容: particle

删除的内容: , 1999

删除的内容: particles

已上移 [10]: Atmos.

已上移 [5]: Environ., 34,

删除的内容: . and Waldhoff, S. T.: Present and future emissions of air pollutants in China: SO₂, NO_x, and CO,

带格式的: 字体: AdvOT863180fb, 字体颜色: 黑色

删除的内容: 3, 363-374, 2000. . Streets, D. G

954 [Sun, L., Xue, L. K., Wang, T., Gao, J., Ding, A. J., Cooper, O. R., Lin, M. Y., Xu, P. J., Wang, Z., Wang, X. F., Wen, L.,](#)
955 [Zhu, Y. H., Chen, T. S., Yang, L. X., Wang, Y., Chen, J. M., and Wang, W. X.: Significant increase of summertime](#)
956 [ozone at Mount Tai in Central Eastern China, *Atmos. Chem. Phys.*, 16, 10637-10650, 2016.](#)

957 Sun, G., Yao, L., Jiao, L., Shi, Y., Zhang, Q., Tao, M., Shan, G., and He, Y.: Characterizing PM_{2.5} pollution of a subtropical
958 metropolitan area in China, *Atmos. Climate. Sci.*, 3, 11, 2013.

959 Trainer, M., Parrish, D. D., Buhr, M. P., Norton, R. B., Fehsenfeld, F. C., Anlauf, K. G., Bottenheim, J. W., Tang, Y. Z.,
960 Wiebe, H. A., Roberts, J. M., Tanner, R. L., Newman, L., Bowersox, V. C., Meagher, J. F., Olszyna, K. J., Rodgers, M.
961 O., Wang, T., Berresheim, H., Demerjian, K. L., and Roychowdhury, U. K.: Correlation of O₃ with NO_y in
962 photochemically aged air, *J. Geophys. Res.*, 98, 2917-2925, 1993.

963 Wang, R., Tao, S., Ciais, P., Shen, H. Z., Huang, Y., Chen, H., Shen, G. F., Wang, B., Li, W., Zhang, Y. Y., Lu, Y., Zhu, D.,
964 Chen, Y. C., Liu, X. P., Wang, W. T., Wang, X. L., Liu, W. X., Li, B. G., and Piao, S. L.: High-resolution mapping of
965 combustion processes and implications for CO₂ emissions, *Atmos. Chem. Phys.*, 13, 10, 5189-5203, 2013.

966 Wang, G., Huang, L., Gao, S., Gao, S., and Wang, L.: Characterization of water-soluble species of PM₁₀ and PM_{2.5} aerosols
967 in urban area in Nanjing, China, *Atmos. Environ.*, 36, 1299-1307, 2002.

968 Wang, G., Wang, H., Yu, Y., Gao, S., Feng, J., Gao, S., and Wang, L.: Chemical characterization of water-soluble
969 components of PM₁₀ and PM_{2.5} atmospheric aerosols in five locations of Nanjing, China, *Atmos. Environ.*, 37, 2893-
970 2902, 2003.

971 Wang, T., Cheung, V. T. F., Anson, M., and Li, Y. S.: Ozone and related gaseous pollutants in the boundary layer of eastern
972 China: overview of the recent measurements at a rural site, *Geophys. Res. Lett.*, 28, 2373-2376, 2001.

973 Wang, T., Wong, C. H., Cheung, T. F., Blake, D. R., Arimoto, R., Baumann, K., Tang, J., Ding, G. A., Yu, X. M., Li, Y. S.,
974 Streets, D. G., and Simpson, I. J.: Relationships of trace gases and aerosols and the emission characteristics at Lin'an, a
975 rural site in eastern China, during spring 2001, *J. Geophys. Res.*, 109, 19, 2004.

976 Wang, Y., Ying, Q., Hu, J., and Zhang, H.: Spatial and temporal variations of six criteria air pollutants in 31 provincial
977 capital cities in China during 2013-2014, *Environ. Int.*, 73, 413-422, 2014.

978 Wang, Y. Q., Zhang, X. Y., Arimoto, R., Cao, J. J., and Shen, Z. X.: The transport pathways and sources of PM₁₀ pollution
979 in Beijing during spring 2001, 2002 and 2003, *Geophys. Res. Lett.*, 31, L14110, 2004.

980 Wu, J., Xu, C., Wang, Q., and Cheng, W.: Potential sources and formations of the PM_{2.5} pollution in urban Hangzhou,
981 *Atmosphere*, 7, 100, 2016a.

982 Wu, Y., Hu, M., Zeng, L., Dong, H., Li, X., Lu, K., Lu, S., Yang, Y., and Zhang, Y.: Seasonal variation of trace gas
983 compounds and PM_{2.5} observed at an urban supersite in Beijing, *EGU General Assembly Conference Abstracts*, 12409,
984 2016b.

985 [Xue, L. K., Wang, T., Gao, J., Ding, A. J., Zhou, X. H., Blake, D. R., Wang, X. F., Saunders, S. M., Fan, S. J., Zuo, H. C.,](#)
986 [Zhang, Q. Z., and Wang, W. X.: Ground-level ozone in four Chinese cities: precursors, regional transport and](#)
987 [heterogeneous processes, *Atmos. Chem. Phys.*, 14, 13175-13188, 2014.](#)

已上移 [11]: H.,

删除的内容: Xu, H.

已上移 [9]: Adv.

删除的内容: Pu, J. J., He, J., Liu, J., Qi, B., and Du, R.-G.: Characteristics of atmospheric compositions in the background area of Yangtze River Delta during heavy air pollution episode,

删除的内容: Meteor., 1-13, 2016. .

997 | [Xue, L. K., Wang, T., Louie, P. K. K., Luk, C.W. Y., Blake, D. R., Xu, Z.: Increasing external effects negate local efforts to](#)
998 | [control ozone air pollution: a case study of Hong Kong and implications for other Chinese cities. Environ. Sci. Tech.,](#)
999 | [48\(18\), 10769-10775, 2014.](#)

1000 | Yang, L. X., Cheng, S. H., Wang, X. F., Nie, W., Xu, P. J., Gao, X. M., Yuan, C., and Wang, W. X.: Source identification
1001 | and health impact of PM_{2.5} in a heavily polluted urban atmosphere in China, Atmos. Environ., 75, 265-269, 2013.

1002 | Yu, S. C., Zhang, Q. Y., Yan, R. C., Wang, S., Li, P. F., Chen, B. X., Liu, W. P., and Zhang, X. Y.: Origin of air pollution
1003 | during a weekly heavy haze episode in Hangzhou, China, Environ. Chem. Lett., 12, 543-550, 2014.

1004 | Zhang, H. L., Li, J. Y., Ying, Q., Yu, J. Z., Wu, D., Cheng, Y., He, K. B., and Jiang, J. K.: Source apportionment of PM_{2.5}
1005 | nitrate and sulfate in China using a source-oriented chemical transport model, Atmos. Environ., 62, 228-242, 2012.

1006 | Zhang, L. M., Gong, S. L., Padro, J., and Barrie, L.: A size segregated ~~particulate~~ dry deposition scheme for an atmospheric
1007 | aerosol module, Atmos. Environ., 35, 549-560, 2001.

1008 | Zhang, R. Jing, J., Tao, J., Hsu, S. C., Wang, G., Cao, J., Lee, C. S. L., Zhu, L., Chen, Z., Zhao, Y., and Shen, Z.: Chemical
1009 | characterization and source apportionment of PM_{2.5} in Beijing: seasonal perspective, Atmos. Chem. Phys., 13, 7053-
1010 | 7074, 2013.

1011 | Zhang, R. Y., Suh, I., Zhao, J., Zhang, D., Fortner, E. C., Tie, X. X., Molina, L. T., and Molina, M. T.: Atmospheric new
1012 | ~~particulate~~ formation enhanced by organic acids, Science, 304, 5676, 1487-1490, 2004.

1013 | Zhang, Q., Yuan, B., Shao, M., Wang, X., Lu, S., Lu, K., Wang, M., Chen, L., Chang, C.-C., and Liu, S. C.: Variations of
1014 | ground-level O₃ and its precursors in Beijing in summertime between 2005 and 2011, Atmos. Chem. Phys., 14, 6089-
1015 | 6101, 2014.

1016 | Zhang, Q., Streets, D. G., Carmichael, G. R., He, K. B., Huo, H., Kannari, A., Klimont, Z., Park, I. S., Reddy, S., Fu, J. S.,
1017 | Chen, D., Duan, L., Lei, Y., Wang, L. T., and Yao, Z. L.: Asian emissions in 2006 for the NASA INTEX-B mission,
1018 | Atmos. Chem. Phys., 9, 5131-5153, 2009.

1019 | Zhong, Q. R., Huang, Y., Shen, H. Z., Chen, Y. L., Chen, H., Huang, T. B., Zeng, E. Y., and Tao, S.: Global estimates of
1020 | carbon monoxide emissions from 1960 to 2013, Environ. Sci. Pollut. Res., 24, 864-873, 2014.

1021

删除的内容: particulate

删除的内容: particulate

带格式的: 下标

1024 Table 1 Statistics of general meteorological parameters at NRCS for the period during January- December 2013*.

Month	Temperature (°C)	RH (%)	Wind Speed (m s ⁻¹)	Rainfall (mm)	Pressure (Pa)	Visibility (m)
Jan.	4.5 ± 3.4	76 ± 9	1.9	24.9	10221.6	2566.0
Feb.	7.0 ± 4.3	81 ± 6	2.3	66.8	10197.2	3511.8
Mar.	12.3 ± 4.2	67 ± 15	2.7	115.9	10140.5	5459.1
Apr.	16.9 ± 3.9	56 ± 17	2.6	98.1	10095.3	7587.8
May	23.0 ± 3.0	69 ± 13	2.1	121.3	10045.8	6118.9
Jun.	24.7 ± 3.1	78 ± 7	2.0	346	10013.0	5693.5
Jul.	32.3 ± 1.6	51 ± 7	2.8	9.3	9997.8	17011.0
Aug.	31.3 ± 2.7	58 ± 14	2.6	212.1	10001.7	13958.3
Sep.	25.0 ± 2.7	73 ± 11	2.3	49.4	10015.2	9584.7
Oct.	19.3 ± 2.8	73 ± 11	2.5	331	10146.1	7551.8
Nov.	13.5 ± 3.9	68 ± 16	1.9	32.6	10178.8	5759.2
Dec.	6.3 ± 3.6	64 ± 15	2.0	82.7	10208.6	3941.2

1025 *Note: average values for air temperature (T), relative humidity (RH), wind speed (WS), pressure, and visibility and
 1026 accumulated monthly value for rainfall, respectively.

1027

删除的内容: 2

删除的内容: 24.5

1030 Table 2 Mean species levels for different seasons and different time of day and comparisons with other previous data
 1031 reported in typical regions in China.

Species	Areas	Location	Period	The whole day			Day time (08:00-17:00)			Night time (18:00-07:00)		
				Mean	SD	Max	Mean	SD	Max	Mean	SD	Max
PM _{2.5} ($\mu\text{g m}^{-3}$)	This study		DJF	74.2	49.3	406.4	75.1	50.5	406.4	73.6	48.4	325.5
			MAM	47.1	26.2	201.1	47.7	26.6	201.1	46.7	25.9	154.0
			JJA	34.6	22.5	181	35.1	25.7	181.0	34.3	20.0	139.6
			SON	52.5	34.4	272.4	51.7	33.3	238.1	53.1	35.1	272.4
	YRD		^a Xiacheng District, Hangzhou (Sep.-Nov. 2013) monthly mean: $69 \mu\text{g m}^{-3}$									
			^b NRCS, Hangzhou (2012) annual mean: $50.0 \mu\text{g m}^{-3}$									
			^c Hangzhou (Sep. 2010-Nov. 2011 during non-raining days) annual average: $106\text{-}131 \mu\text{g m}^{-3}$									
	BTH		^d Nine sites in Nanjing (2013) AM: $55\text{-}60 \mu\text{g m}^{-3}$, JJA: $30\text{-}60 \mu\text{g m}^{-3}$, SON: $55\text{-}85 \mu\text{g m}^{-3}$									
			^e Nanjing (Mar. 2013-Feb. 2014) annual mean: $75 \pm 50 \mu\text{g m}^{-3}$									
			^e Shanghai (Mar. 2013-Feb. 2014) annual mean: $56 \pm 41 \mu\text{g m}^{-3}$									
PRD		^e Beijing (Mar. 2013-Feb. 2014) annual mean: $87 \pm 67 \mu\text{g m}^{-3}$										
		^e Guangzhou (Mar. 2013-Feb. 2014) annual mean: $52 \pm 28 \mu\text{g m}^{-3}$										
PM ₁₀ ($\mu\text{g m}^{-3}$)	This study		DJF	113.1	71.7	589.6	115.3	73.6	589.6	111.5	70.4	481.6
			MAM	77.1	42.3	484.1	79.3	41.0	249.1	75.6	43.2	484.1
			JJA	54.9	31.6	231.4	55.7	34.8	231.4	54.4	29.2	183.8
			SON	85.6	51.2	344.2	84.8	48.6	341.3	86.1	53.0	344.2
	YRD		^e Hangzhou (Mar. 2013-Feb. 2014) annual mean: $98 \pm 59 \mu\text{g m}^{-3}$									
			^c Hangzhou (Sep. 2010-Nov. 2011 during non-raining days) annual average: $127\text{-}158 \mu\text{g m}^{-3}$									
			^f Hangzhou (Sep. 2001-Aug. 2002) annual mean: $119.2 \mu\text{g m}^{-3}$									
	BTH		^e Nanjing (Mar. 2013-Feb. 2014) annual mean: $134 \pm 73 \mu\text{g m}^{-3}$									
			^e Shanghai (Mar. 2013-Feb. 2014) annual mean: $80 \pm 47 \mu\text{g m}^{-3}$									
			^e Beijing (Mar. 2013-Feb. 2014) annual mean: $109 \pm 62 \mu\text{g m}^{-3}$									
PRD		^e Guangzhou (Mar. 2013-Feb. 2014) annual mean: $72 \pm 35 \mu\text{g m}^{-3}$										
O ₃ (ppbv)	This study		DJF	13.8	13.1	70.9	17.7	14.1	70.9	10.2	10.9	58.5
			MAM	29.8	24.0	141.2	42.4	27.3	141.2	20.0	15.1	105.9
			JJA	31.3	26.0	145.4	48.8	26.6	145.4	18.2	15.8	118.7
			SON	25.9	22.5	100.1	37.0	25.1	100.1	16.3	14.3	99.5
	YRD		^e Hangzhou (Mar. 2013-Feb. 2014) annual mean: 44 ± 21 ppbv (8 h O ₃)									
			^e Nanjing (Mar. 2013-Feb. 2014) annual mean: 42 ± 20 ppbv (8 h O ₃)									
			^e Shanghai (Mar. 2013-Feb. 2014) annual mean: 48 ± 21 ppbv (8 h O ₃)									
	BTH		^e Beijing (Mar. 2013-Feb. 2014) annual mean: 45 ± 27 ppbv (8 h O ₃)									
	PRD		^e Guangzhou (Mar. 2013-Feb. 2014) annual mean: 45 ± 24 ppbv (8 h O ₃)									
	SO ₂ (ppbv)	YRD	This study	DJF	14.5	10.2	71.2	16.2	10.2	71.2	13.3	10.2

MAM	11.3	9.1	75.1	11.7	9.6	75.1	11.0	8.7	59.3
JJA	8.6	6.5	51.0	8.0	6.3	51.0	9.0	6.6	46.7
SON	9.6	7.2	63.8	10.3	7.1	58.3	9.0	7.3	63.8

^a Hangzhou Xiacheng District (12-19 Oct., 2013) daily mean: 5.7-9.7 ppbv

^c Hangzhou (Mar. 2013-Feb. 2014) annual mean: 9 ±4 ppbv

^c Nanjing (Mar. 2013-Feb. 2014) annual mean: 12 ± 6 ppbv

^c Shanghai (Mar. 2013-Feb. 2014) annual mean: 7 ± 5 ppbv

BTH ^c Beijing (Mar. 2013-Feb. 2014) annual mean: 9 ± 8 ppbv

PRD ^c Guangzhou (Mar. 2013-Feb. 2014) annual mean: 7 ± 3 ppbv

CO (ppmv)	YRD	This study	DJF	1.4	0.7	3.8	1.4	0.7	3.3	1.4	0.7	3.8
			MAM	0.7	0.2	2.2	0.7	0.3	2.2	0.7	0.2	1.7
			JJA	0.5	0.2	2.0	0.5	0.2	1.9	0.5	0.2	2.0
			SON	0.8	0.3	3.4	0.7	0.3	1.9	0.8	0.3	3.4
	^c Hangzhou (Mar. 2013-Feb. 2014) annual mean: 0.7 ±0.3 ppmv											
	^c Nanjing (Mar. 2013-Feb. 2014) annual mean: 0.8 ±0.4 ppmv											
	^c Shanghai (Mar. 2013-Feb. 2014) annual mean: 0.7 ±0.3 ppmv											
	BTH	^c Beijing (Mar. 2013-Feb. 2014) annual mean: 1.1 ± 0.7 ppmv										
	PRD	^c Guangzhou (Mar. 2013-Feb. 2014) annual mean: 0.8 ± 0.2 ppmv										

NO ₂ (ppbv)	YRD	This study	DJF	37.4	20.1	146.9	35.7	19.5	126.3	38.5	20.5	146.9
			MAM	28.7	12.9	94.8	25.3	12.1	94.8	31.0	12.9	87.4
			JJA	17.3	10.2	61.4	13.0	9.2	46.1	20.3	9.7	61.4
			SON	28.4	15.2	94.1	25.1	13.3	86.2	30.7	16.0	94.1
	^c Hangzhou (Mar. 2013-Feb. 2014) annual mean: 13 ±9 ppbv											
	^c Nanjing (Mar. 2013-Feb. 2014) annual mean: 26 ±11 ppbv											
	^c Shanghai (Mar. 2013-Feb. 2014) annual mean: 20 ±9 ppbv											
	BTH	^c Beijing (Mar. 2013-Feb. 2014) annual mean: 25 ±11 ppbv										
	PRD	^c Guangzhou (Mar. 2013-Feb. 2014) annual mean: 24 ±10 ppbv										

NO _x (ppbv)	YRD	This study	DJF	60.5	34.7	199.8	58.0	32.1	168.9	62.3	36.3	199.8
			MAM	40.0	19.8	131.4	36.5	19.2	129.2	42.5	19.8	131.4
			JJA	24.3	14.8	99.6	18.6	14.1	99.6	28.2	14.0	83.1
			SON	41.0	24.3	153.4	36.6	21.1	123.7	44.2	25.8	153.4

NO _y (ppbv)	YRD	This study	DJF	84.7	48.4	295.2	82.4	44.6	263.7	86.4	51.1	295.2
			MAM	66.0	33.6	248.8	62.9	34.6	248.8	68.2	32.8	204.1
			JJA	43.6	27.6	259.5	36.8	29.3	259.5	48.5	25.2	167.7
			SON	70.2	37.9	319.3	65.5	35.6	319.3	73.6	39.1	251.8

^g Nanjing SORPES 2013 monthly mean: 30-70 ppbv

^h Shanghai May-June 2005 daily mean: 24-39 ppbv

BTH ^a Beijing 2011-2015 annual mean: 54.6 ± 4.7 ppbv

YRD ^h Guangzhou Apr.-May 2004: 24-52 ppbv

1032 ^a Wu et al. (2016a); ^b Qi et al. (2015); ^c Sun et al. (2013); ^d Chen et al. (2016); ^e Wang et al. (2014); ^f Cao et al. (2009); ^g Ding
1033 et al. (2013); ^h Xue et al. (2014)

1034 Table 3 Mean concentrations of PM_{2.5} (µg m⁻³) and other trace gases (ppmv unit for CO but ppbv for other gases) in the
 1035 identified trajectory clusters within four season period, together with the percentages of each trajectory cluster.

Season	Cluster	Percent (%)	PM _{2.5}	O ₃	SO ₂	CO	NO _x
Spring	1	12.05	45.0	28.3	10.7	0.7	38.3
	2	16.58	44.3	31.6	13.2	0.7	39.1
	3	16.03	35.3	30.5	9.7	0.6	34.5
	4	42.66	52.4	23.2	11.4	0.8	42.5
	5	5.53	38.2	34.2	11.2	0.7	37.9
	6	7.16	58.1	34.2	11.9	0.8	43.8
Summer	1	8.42	51.5	24.6	7.9	0.8	29.2
	2	8.61	34.2	35.2	9.2	0.5	22.8
	3	22.55	24.0	28.7	7.9	0.4	21.7
	4	31.34	38.2	36.8	9.1	0.5	24.4
	5	19.38	38.7	27.2	8.9	0.6	28.7
	6	9.69	22.4	26.7	7.5	0.4	17.6
Autumn	1	23.63	42.1	27.4	9.9	0.7	36.9
	2	32.51	50.7	24.6	8.2	0.8	39.4
	3	8.33	21.7	19.8	8.0	0.5	22.0
	4	7.78	68.6	34.8	8.4	0.8	38.8
	5	11.90	49.9	22.6	10.1	0.7	40.8
	6	15.84	79.6	21.6	12.9	0.9	62.0
Winter	1	7.13	60.9	16.6	15.4	1.3	53.7
	2	24.26	83.3	14.4	15.9	1.4	65.4
	3	16.39	47.3	14.0	11.9	1.1	42.7
	4	21.76	75.9	11.9	13.5	1.5	63.1
	5	16.76	67.0	11.7	13.1	1.5	53.7
	6	13.70	102.1	14.4	16.9	1.4	81.0

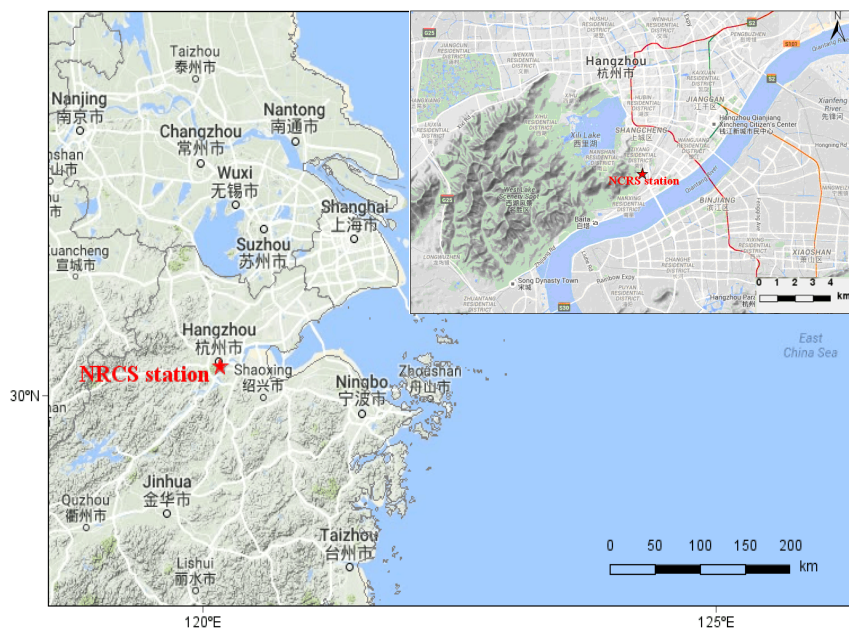
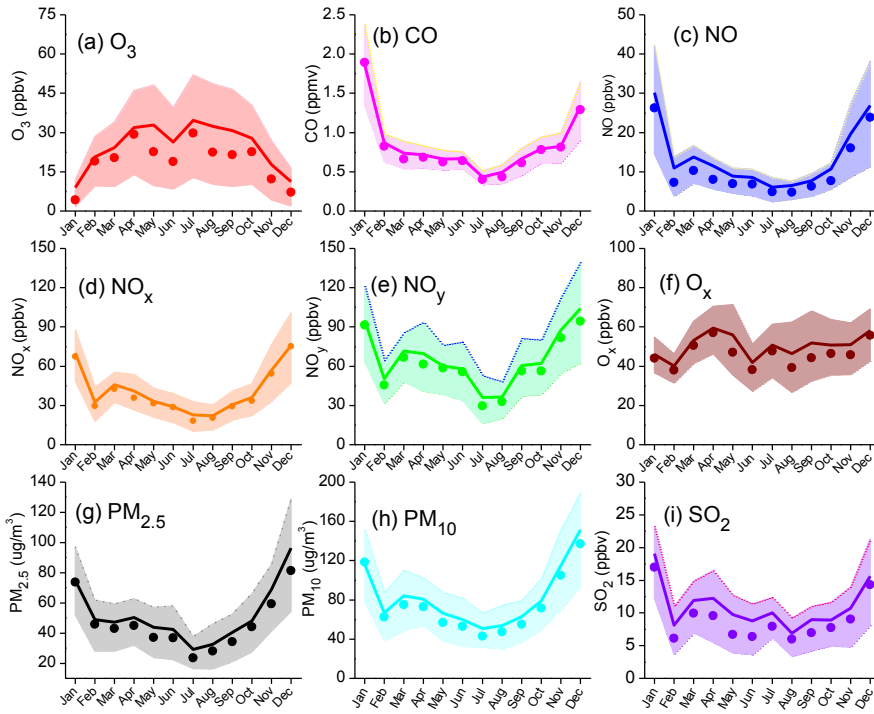


Fig. 1. Location of NRCS station in YRD region (left) and in the city of Hangzhou (right top).

1036
1037



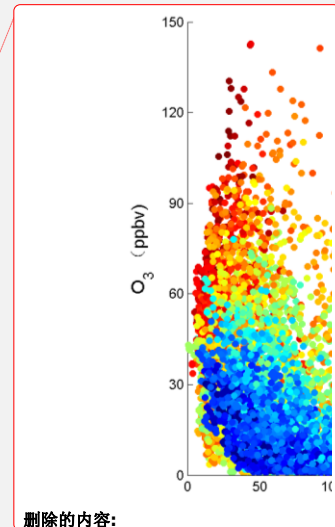
1038

1039 Fig. 2. Seasonal variations of atmospheric O₃ (a), CO (b), NO (c), NO_x (d), NO_y (e), O_x (f), PM_{2.5} (g), PM₁₀ (h), and SO₂ (i).

1040 Bold solid lines are the monthly averages, solid circles are the median values, and thin lines represent percentiles of 75% and

1041 25%.

1042 |



删除的内容:

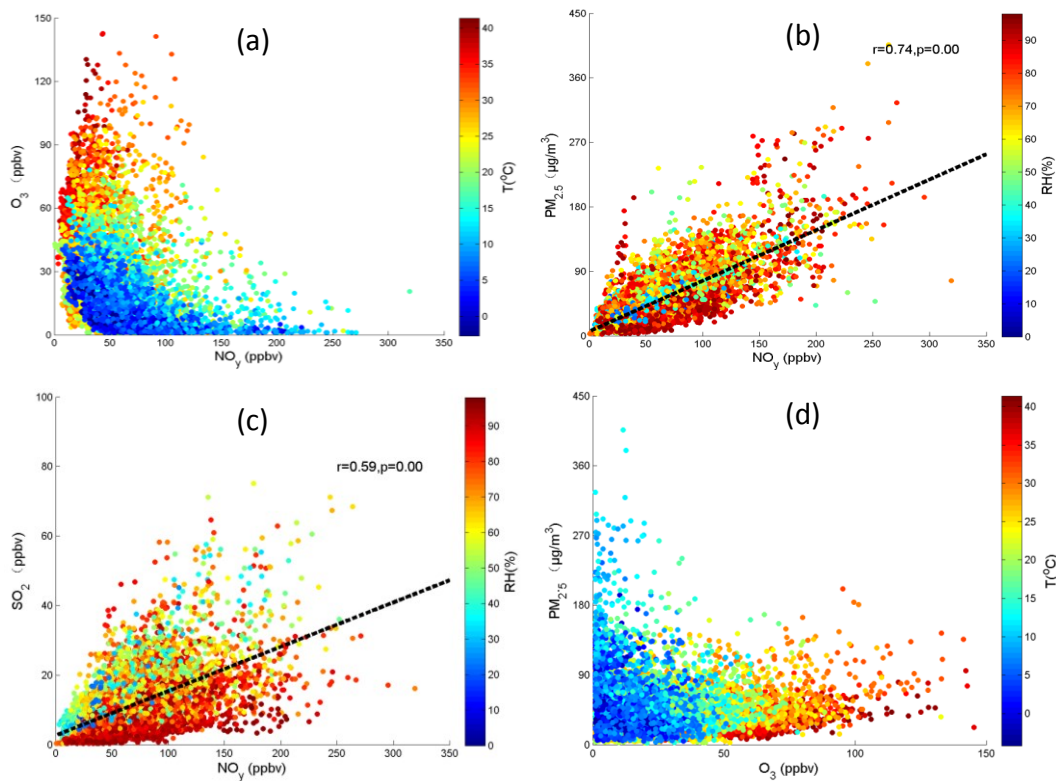


Fig. 3. Scatter plots of NO_y with O_3 (NO_y - O_3) coded with air temperature, (a), NO_y - $\text{PM}_{2.5}$ coded with relative humidity, (b), NO_y - SO_2 coded with relative humidity (c), and O_3 - $\text{PM}_{2.5}$ coded with air temperature (d).

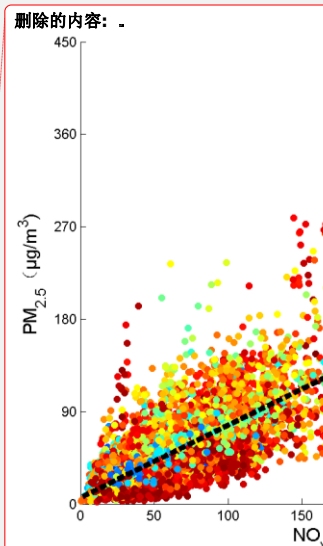
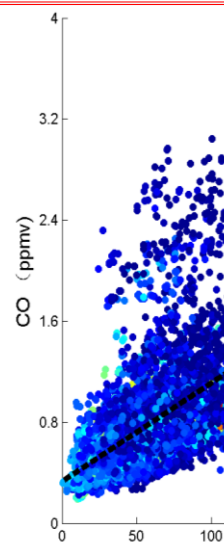


Fig. 4. Scatter plots of NO_y with

删除的内容: -
带格式的: 两端对齐, 段落间距段后: 0.5 行



删除的内容:

1044
1045
1046
1047
1048
1049
1050
1051
1052

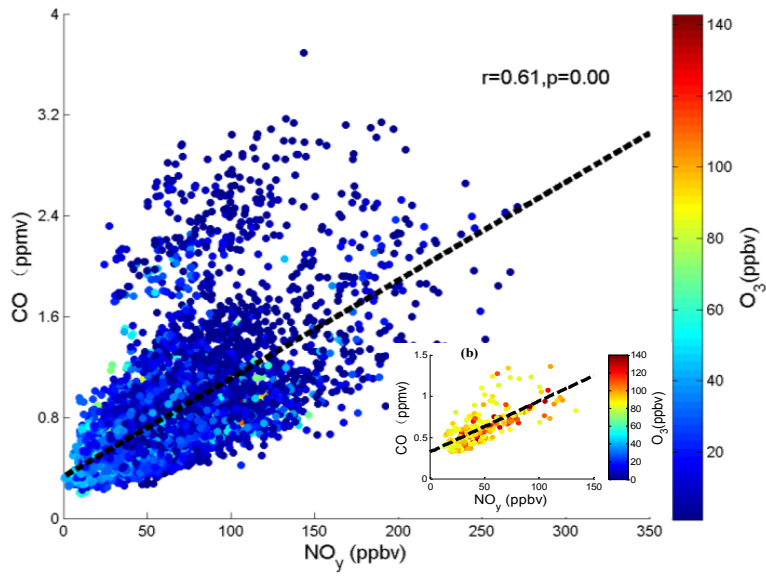


Fig. 4. Scatter plots of NO_y with CO coded with O₃ mixing ratios, along the subpicture (b) showing the scatter with O₃ mixing ratios above 80 ppbv.

删除的内容: 6

1061
1062
1063
1064

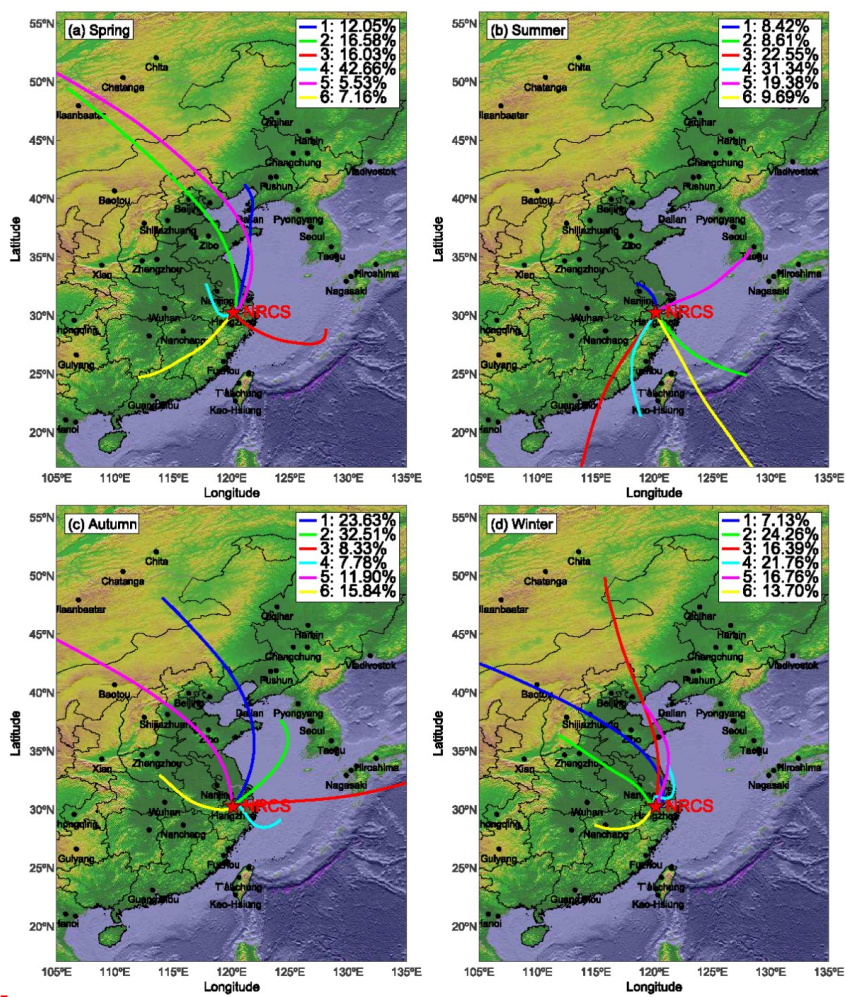
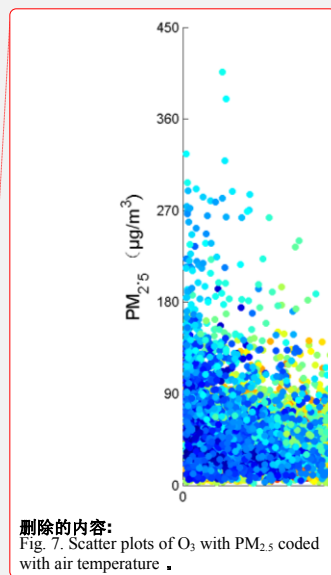
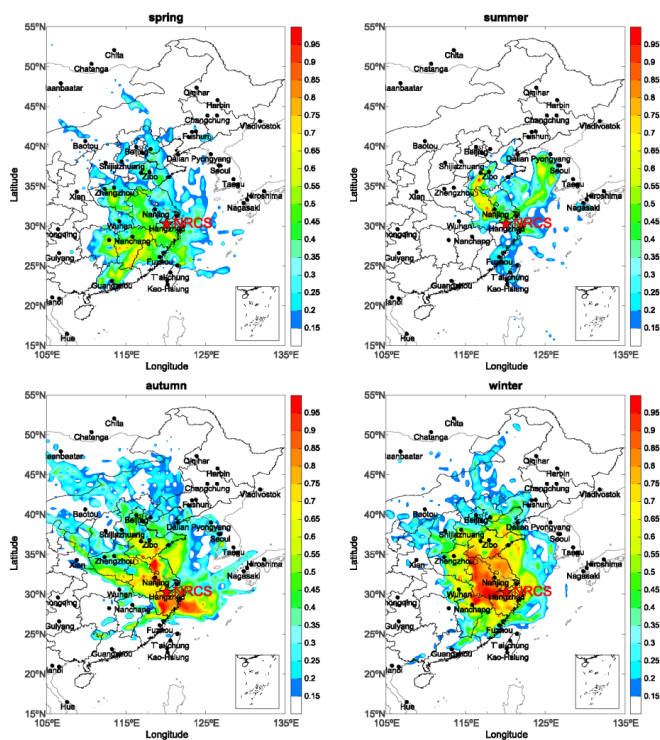


Fig. 5. Seasonal cluster analysis of the 72-h air mass back trajectories starting at 100 m from NRCS site in Hangzhou.



删除的内容:
Fig. 7. Scatter plots of O₃ with PM_{2.5} coded with air temperature .

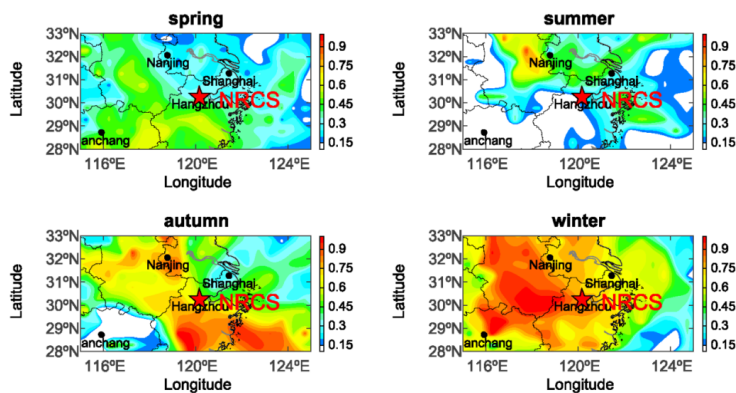
删除的内容: 8



1072

1073 | Fig. 6a. Seasonal weighted potential source contribution function (WPSCF) maps of $PM_{2.5}$ in Hangzhou. The sampling site is
 1074 | marked in pentacle and the WPSCF values are displayed in color.

删除的内容: 9a



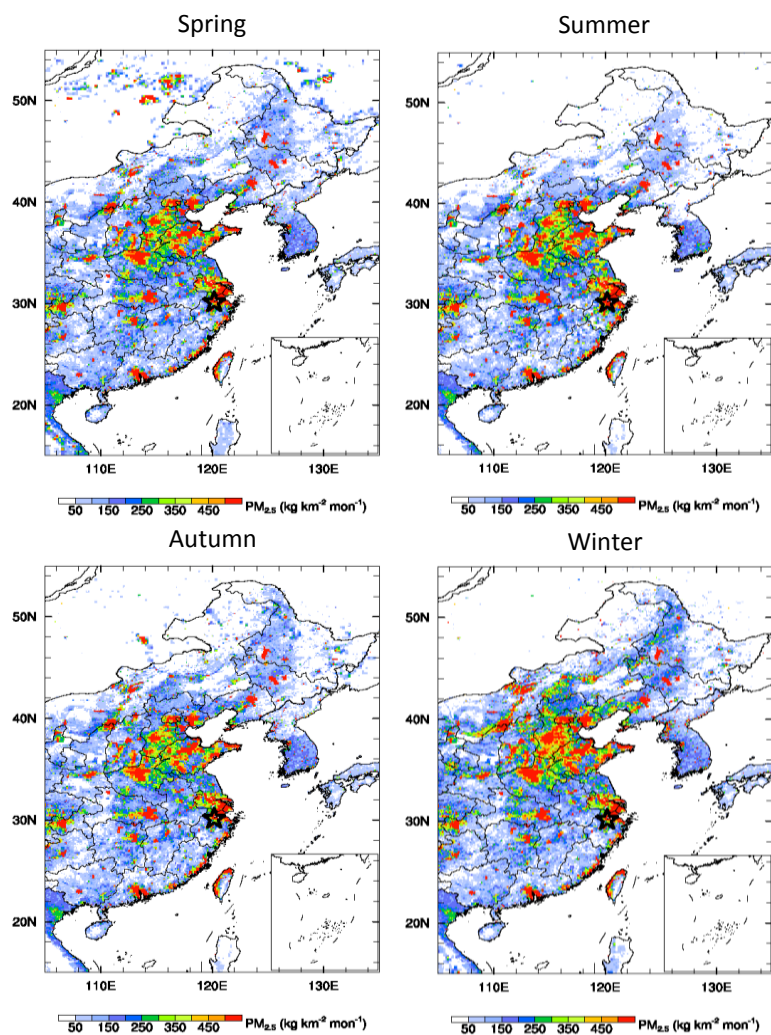
1075

1076 |

Fig. 6b. The zoomed view of Fig. 6a.

删除的内容: 9b

删除的内容: 9a



1080
 1081 | Fig. 6c. Seasonal and spatial distributions of PM_{2.5} emissions (kg km² mon⁻¹) at the surface layer in China. The sampling site
 1082 is marked in pentacle.

删除的内容: %c

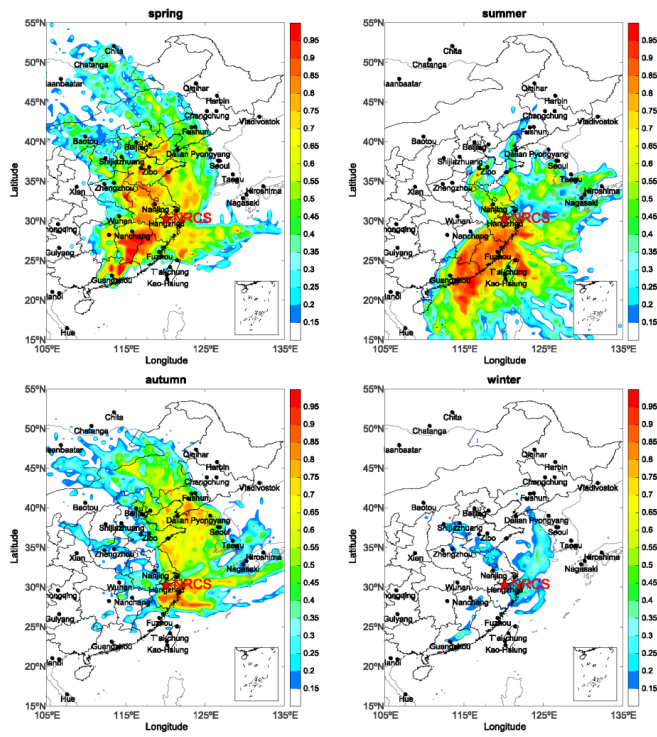


Fig. 7a. Same as Fig. 6a but for O_3

删除的内容: 10a

删除的内容: 9a

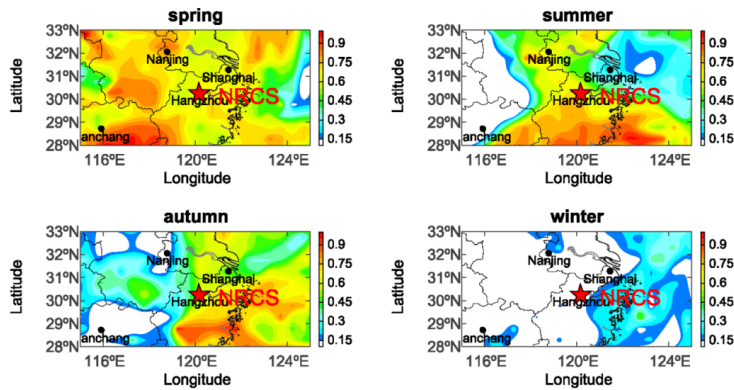


Fig. 7b The zoomed view of Fig. 7a

删除的内容: 10b

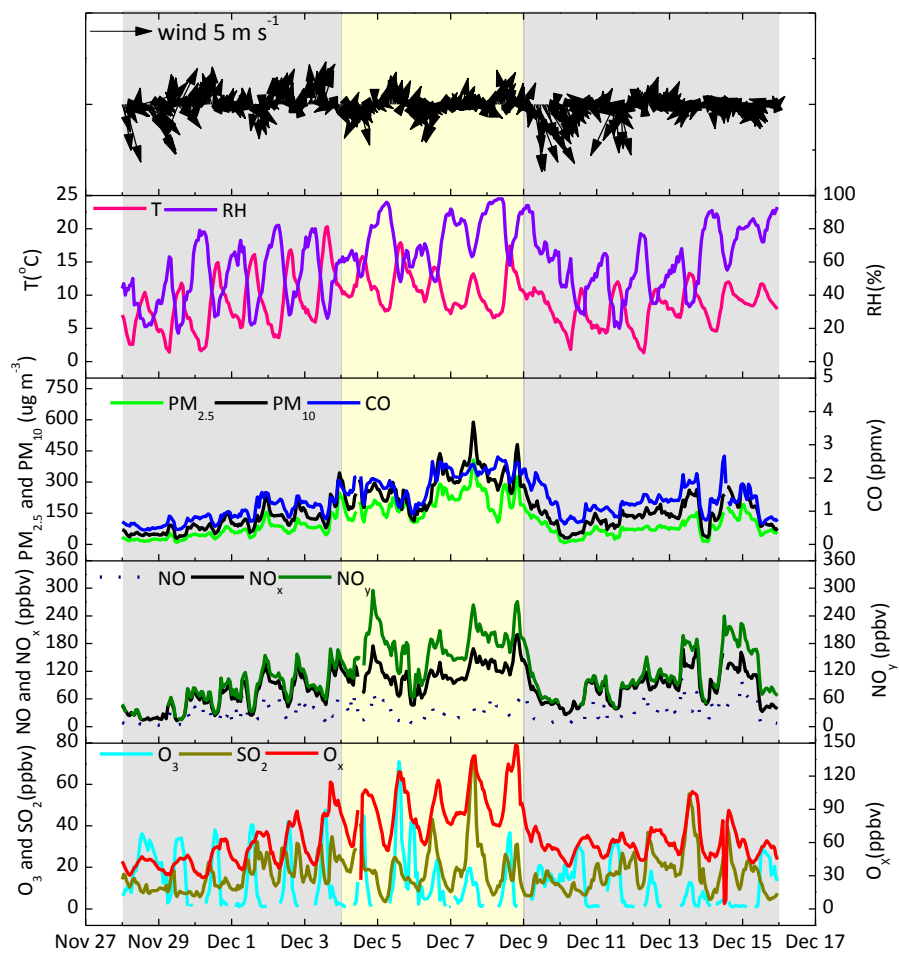
删除的内容: 10a

1084

1085

1086

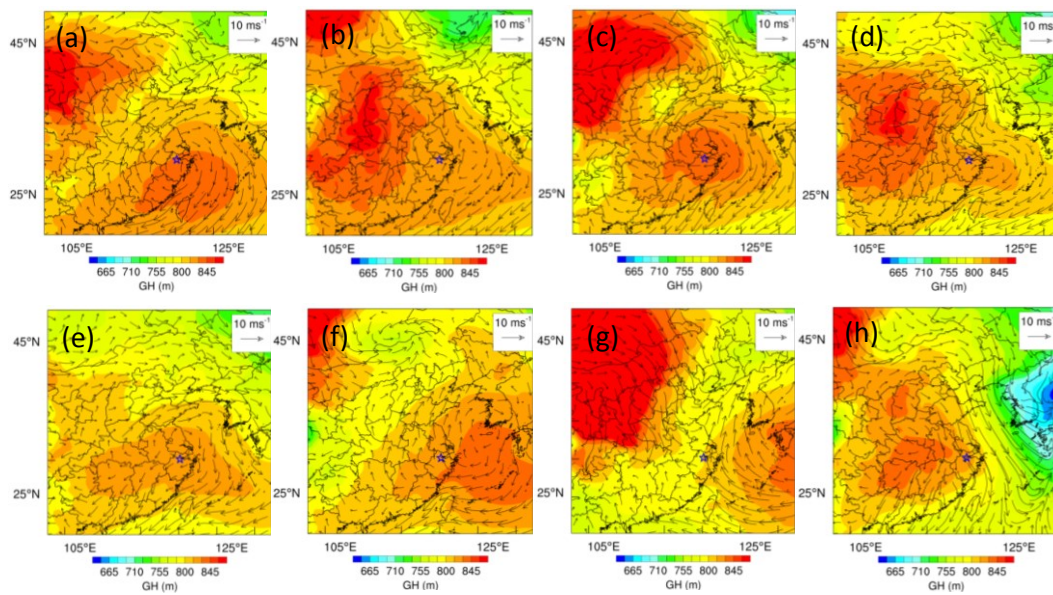
1087



1092

1093 | Fig. 8. Time series of meteorological parameters and chemical species before, during, and after haze period. The gray shaded
 1094 area indicates the Phase I (28 Nov.-3 Dec.) and II (10-12 Dec.) and the orange shaded area represents haze events Phase III
 1095 (2-9 Dec.) and IV (13-15 Dec.).

删除的内容: 11



1097

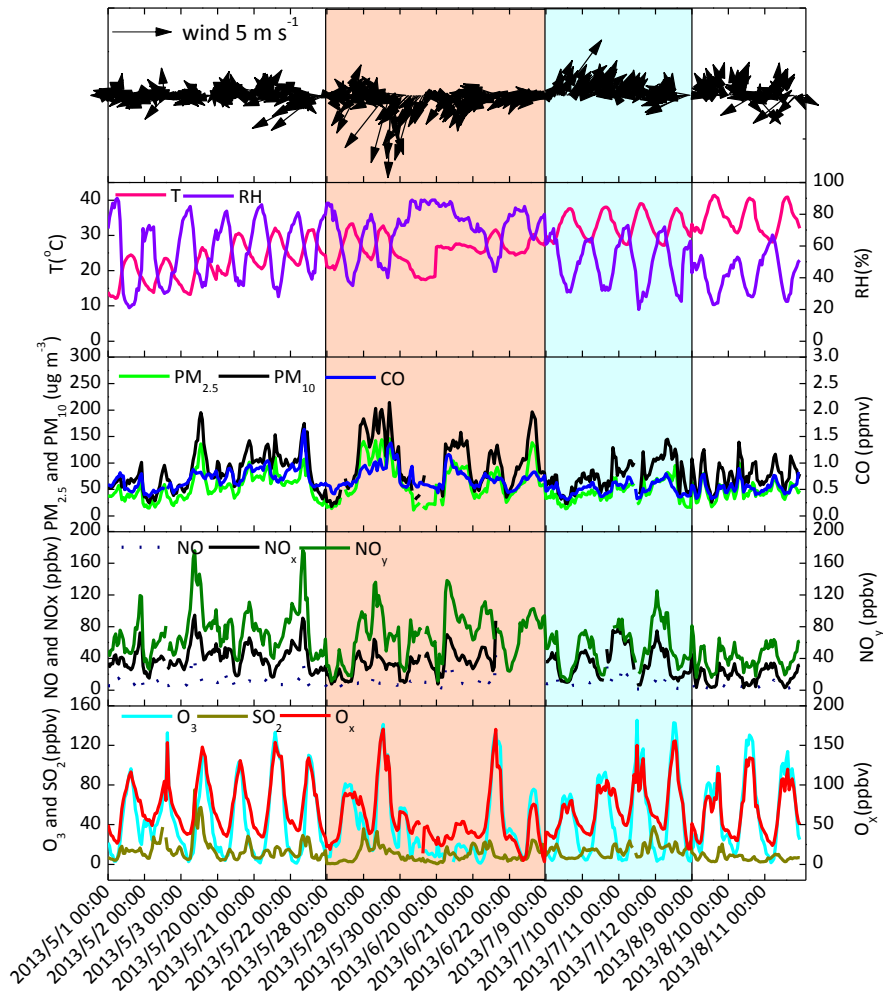
1098

1099

1100

Fig. 9. The Geopotential Height Field (GH) (indicated by color bars) and Wind Field (WF) (black vectors) for 925 hPa at 20:00 LT during 2-9 December, 2013. Fig. 12a-d and Fig. 12e-h represent for 2-5 December and 6-9 December from left to right on the top and bottom, respectively. The NRCS station was marked by pentagram.

删除的内容: 12



1102

1103 | Fig. 10. Same as Fig. 8 but during photochemical pollution period. The orange shaded area represents the Phase I (28-30
 1104 May and 20-22 June), the cyan shaded area indicates the Phase II (9-12 July), and the other area represents the Phase III (1-3
 1105 May, 20-22 May, and 9-11 August)

删除的内容: 13

删除的内容: 11